國立臺灣大學工學院環境工程學研究所

碩士論文

Graduate Institute of Environmental Engineering

College of Engineering

National Taiwan University

Master Thesis

利用紫外光活化過硫酸鹽降解 4-甲基亞苄基樟腦

Ultraviolet light-activated persulfate oxidation of 4-methylbenzylidene camphor

謝松娟

Sung-Chuan Hsieh

指導教授: 林郁真 博士

Advisor: Angela Yu-Chen Lin, Ph.D.

中華民國 108 年 6 月

June, 2019

doi:10.6342/NTU201901036

國立臺灣大學碩士學位論文

口試委員會審定書

（利用紫外光活化過硫酸鹽降解 4-甲基亞苄基樟腦）

(Ultraviolet light-activated persulfate oxidation of 4-methylbenzylidene camphor)

本論文係謝松娟君(學號 R06541112)在國立臺灣大學環境工程學研究所完成之碩（博）士學位論文，於民國 108 年 6 月 17 日承下列考試委員審查通過及口試及格，特此證明

論文審查委員：

林郁真博士
國立台灣大學環境工程學研究所教授

于昌平博士
國立台灣大學環境工程學研究所副教授

林逸彬博士
國立台灣大學環境工程學研究所副教授

指導教授：

所　　長：

致謝

歷經兩年的時間，我終於完成我的碩士論文，這一路走來並非一帆風順，無論是課業或是實驗都曾使我感到挫敗，然而每每遇到困難時，身旁的人總會不吝嗇地向我伸出援手，帶我跨過每一道關卡，除了感到幸運之外，對於他們的幫助我也總是懷抱著一顆感恩的心。

首先要先感謝曾經在實驗室的每一個夥伴 (至演、姿伃、俊宇、欣瑜、冠宇、怡瑄、坤霖、昆圃、昱蓉、宥翔、政憲、明季、明皓)，在過去的日子包容我的不足，在做實驗或上機時互相體諒及幫忙，你們每一個人不管是直接亦或是間接，都著實地成為了我論文中的小螺絲；接著要特別感謝 Webber 學長，從我碩二開始，就不停地麻煩學長幫我看數據並討論，到了最後更是以我沒有想像到的速度在幫我修改論文，真的非常謝謝學長的幫忙，讓我能順利地完成口試。

再來我要感謝我的好朋友 (妤馨、詩婷、子綺)，雖然他們各個都在不同的城市，但卻總是在我遇到困難的第一時間，接受到我不好的情緒，儘管如此他們總是用盡所有的耐心在鼓勵我且陪伴我；還想要感謝我的爸爸媽媽，無論我做什麼決定，他們總是沒有第二句話地百分之百支持我，讓我有充足的發揮空間，謝謝你們每一個人成為了我心中最強壯的後盾。

最後，我想感謝林郁真老師在兩年前收我當學生，還讓只是碩一的我有參加研討會的機會，老師嚴謹又不失關心地指導，讓我有很開心的碩班生活，而在畢業典禮時對我說的話，也讓我更有自信去面對接下來生活。謝謝您。

doi:10.6342/NTU201901036

摘要

4-甲基亞苄基樟腦 (4-MBC) 為常添加於防曬乳的成分之一，並且已有研究指出 4-MBC 會影響雌激素的活性。由於傳統污水處理廠無法有效地去除 4-MBC，因此近年來於許多環境水體中皆檢測出 ng/L 到 μg/L 範圍殘留濃度的 4-MBC。而利用紫外光活化過硫酸鹽是目前認為具前景的高級氧化處理程序，亦有許多研究指出此處理程序能有效去除污水處理廠中難以被去除的有機污染物。因此本研究探討利用紫外光(254 nm)活化過硫酸鹽以降解水體中的 4-MBC。並以瞭解反應機制、主要參與反應之自由基、降解副產物及途徑、毒性變化及實際應用等面向為主要研究目標。

此處理程序在過硫酸鹽濃度範圍於 4.2 μM 到 42 μM 間皆符合擬一階動力學反應；過硫酸鹽濃度亦與反應速率常數呈正線性關係(R^2=0.997)。4-MBC 在單純只照射紫外光的情況下，只會於 E 型異構物與 Z 型異構物之間轉換並不會降解。然而，在 4-MBC 濃度 0.39 μM、過硫酸鹽濃度 42 μM、反應溶液 pH 值為 7 之條件下，本系統能有效地在 6 分鐘內達到 90%的 4-MBC 去除率，此成效遠優於使 4-MBC 在單純只照射紫外光及在過硫酸鹽氧化反應下降解。此外，反應速率常數於酸性 (pH 5) 及中性情況下為 11.8×10^{-2} min^{-1} 到 11.0×10^{-2} min^{-1} 之範圍，然而於鹼性 (pH 9) 條件下則會大幅降低至 6.8×10^{-2} min^{-1}。

藉由自由基抑制與競爭動力學實驗結果發現，在此處理程序中硫酸根自由基

doi:10.6342/NTU201901036

(SO_4^{-}•) 為主要與 4-MBC 反應之自由基，而 SO_4^{-}•與 4-MBC 的二階反應常數經估算為 $(2.95 \pm 0.05) \times 10^9\ M^{-1}\ s^{-1}$。此外，所添加的過硫酸鹽於反應後之十分鐘內皆轉換為硫酸根離子。而 4-MBC 於降解過程將遵循兩種反應途徑：羥基化與去甲基化，並分別生成降解副產物 P1 ($C_{18}H_{22}O_2$, m/z = 271.1587) 與 P2 ($C_{17}H_{22}O$, m/z = 242.2030)。另外經由費氏弧菌毒性試驗顯示，經由紫外光活化過硫酸鹽程序處理後溶液的毒性於反應的前 20 分鐘會不斷上升，且維持相同的毒性一段時間後才開始下降。經由毒性變化與副產物生成之數據結果得以推斷，4-MBC 在反應結束前並沒有被完全礦化，且於反應的過程中生成尚未被發現且毒性比 4-MBC 還高同時亦更具光敏性之降解副產物。另一方面，此處理程序於實際泳池水中之 4-MBC 降解效率會從原先的 93%去除率下降至 48%，推測水中氯離子是造成此現象之主因。因此，未來若欲將此方法應用至實際污水處理，先行過濾無機離子的是重要的一個程序。

關鍵字: 防曬劑、4-甲基亞苄基樟腦、紫外光、過硫酸鹽

doi:10.6342/NTU201901036

Abstract

4-Methylbenzylidene camphor (4-MBC), a widely used UV filter, has been reported to show estrogenic activity. Owing to insufficient removal in conventional wastewater treatment plants, 4-MBC has been widely detected at the level of ng/L to μg/L in the aquatic environment, The UV-activated persulfate (UV/persulfate) process is a promising and efficient technology that has the potential to remove many recalcitrant organic contaminants. Thus, using the UV/persulfate process to degrade 4-MBC was first evaluated in the present study. The goals of this work were to determine the reaction mechanism, reactive species, transformation byproducts formation and pathways, and change in toxicity and to apply process in an actual water matrix.

4-MBC degradation can be well fitted by pseudo-first-order kinetics; the rate constant and the persulfate dosage have a linear relationship in the persulfate dosage range of 4.2 μM to 42 μM. Under the conditions of $[4\text{-MBC}]_0$ = 0.39 μM, $[\text{persulfate}]_0$ = 42 μM and initial pH = 7, up to 90% of 4-MBC was decomposed within 6 min by the UV/persulfate process, which is advantageous compared to the results obtained using UV irradiation alone and persulfate dark oxidation. Upon UV photolysis alone, 4-MBC experienced only photoisomerization between (E)- and (Z)-4-MBC. The rate constant remained similar, ranging from 11.8×10^{-2} min^{-1} to 11.0×10^{-2} min^{-1}, in acidic (pH 5) and neutral pH, whereas it significantly decreased to 6.8×10^{-2} min^{-1} in basic conditions

doi:10.6342/NTU201901036

(pH 9). Radical scavenging and competition kinetics experiments indicated that SO_4^{-}• exhibited much higher reactivity toward 4-MBC than that of HO•, and the second-order rate constant of SO_4^{-}• with 4-MBC was estimated to be $(2.95 \pm 0.05) \times 10^9$ M^{-1} s^{-1}. Moreover, after 10 min of reaction time, all the added persulfate was completely transformed into sulfate anion. 4-MBC followed transformation pathways including hydroxylation and demethylation, resulting in the generation of the transformation products P1 ($C_{18}H_{22}O_2$, m/z = 271.1587) and P2 ($C_{17}H_{22}O$, m/z = 242.2030), respectively. Microtox® acute toxicity tests with *Vibrio fischeri* indicated that the inhibitory effect continuously increased in the first 20 mins and then remained at the same level for a certain time before starting to decrease. The rising toxicity indicated the formation of unknown transformation products that are more toxic and photolabile than 4-MBC itself, and 4-MBC was not completely mineralized at the end of the reaction. In contrast, the 4-MBC degradation rate was significantly attenuated in outdoor swimming pool water (the removal efficiency decreased from 93% to 48%), which resulted from the high concentration of Cl^{-}. Consequently, removing inorganic anions would be an important pretreatment step if this UV/persulfate process were to be used in real wastewater environments.

Keywords: UV filters, 4-Methylbenzylidene camphor, UV, Persulfate

doi:10.6342/NTU201901036

Contents

doi:10.6342/NTU201901036

doi:10.6342/NTU201901036

List of Figures

doi:10.6342/NTU201901036

doi:10.6342/NTU201901036

doi:10.6342/NTU201901036

List of Tables

doi:10.6342/NTU201901036

Chapter 1 Introduction

1.1 Background

Emerging contaminants are chemicals that have been recently discovered, lack regulatory standards, and potentially give rise to deleterious effects on living organisms at environmentally relevant concentrations [1]. Emerging contaminants encompass various groups of compounds, including pharmaceuticals and personal care products (PPCPs), endocrine-disrupting chemicals (EDCs), persistent organic pollutants (POPs), and nanomaterials, etc. Among these compounds, PPCPs, including numerous chemical classes, are the primary examples of emerging contaminants. Pharmaceuticals are prescribed to prevent or treat human and animal disease, whereas personal care products are used to improve the quality of daily life [2].

Currently, the increasing use of UV filters, a kind of PPCP, has arisen out of growing concern about UV irradiation and skin cancer. UV filters can enter the aquatic environment by two major pathways. One pathway is direct discharge via recreational activities (e.g., swimming), and the other is indirect input via wastewater treatment plants (WWTPs). Owing to the low removal efficiency of conventional WWTPs, a series of UV filters have been detected in wastewaters, surface waters, and seawater [3-14]. In addition, many UV filters show estrogenic and additional hormonal activities [15]. Therefore,

doi:10.6342/NTU201901036

developing an efficient process to eliminate these compounds is necessary.

Advanced oxidation processes (AOPs) were first proposed in 1987 and are defined as processes that involve the generation of sufficient reactive radical species to purify water [16]. AOPs are promising and efficient technologies that have the potential to remove many recalcitrant organic contaminants and can be categorized into ozone-based, UV-based, electrochemical, catalytic, and physical AOPs [17]. Among the various approaches, hydroxyl radical (HO•) is the most commonly generated radical in the most AOPs, while sulfate radical (SO_4^{-}•) has lately arisen as an alternative to HO• due to the stronger oxidation power of SO_4^{-}•. Recently, a large amount of published research regarding the utilization of AOPs to decompose contaminants has been performed at the lab scale [17].

doi:10.6342/NTU201901036

1.2 Objective

Among AOP technologies, SO_4^{-}•-based AOPs have recently been considered to be an effective substitute for HO•-based AOPs due to the higher oxidation potential and longer half-time of SO_4^{-}• than those of HO•, as shown in Table 1 [20-22]. In addition, HO• experiences a much larger self-scavenging effect by its precursor (H_2O_2) compared to that of SO_4^{-}• by its precursor (persulfate) (Eq.1-2) [21, 22].

$$HO\bullet + H_2O_2 \rightarrow H_2O + HO_2\bullet \qquad k = 2.7 \times 10^7 M^{-1}s^{-1} \qquad \text{Eq. 1}$$

$$SO_4^{-}\bullet + S_2O_8^{2-} \rightarrow SO_4^{2-} + S_2O_8^{-}\bullet \qquad k = 6.6 \times 10^5 M^{-1}s^{-1} \qquad \text{Eq. 2}$$

Table 1. Oxidation potential and half-life of hydroxyl radical and sulfate radical.

	HO•	**SO_4^{-}•**
Oxidation potential (V)	1.89−2.72	2.5−3.1
Half-time	10^{-3} μs	30–40 μs

Studies related to 4-MBC removal are rather limited. A previous study reported that the combined effects of TiO_2, H_2O_2, and UVC light achieved 80% degradation of 4-MBC [23]. Both ozonation and adsorption onto activated carbon are effective techniques to remove 4-MBC [24]. However, there has been no research on the degradation of 4-MBC by the UV-activated persulfate (UV/persulfate) process in water. Due to the increasing use of sunscreens and the widespread detection of 4-MBC, this work contributes to the evaluation of 4-MBC degradation in the UV/persulfate process, which can provide useful

doi:10.6342/NTU201901036

information for 4-MBC removal in waters. The specific objectives of this study are as follows.

i. To determine the effects of persulfate dosage and pH on the degradation rate of 4-MBC in the UV/persulfate process.

ii. To identify the dominant reactive species during 4-MBC degradation in the UV/persulfate process.

iii. To understand the final product of persulfate during 4-MBC degradation in the UV/persulfate process.

iv. To explore the transformation products and change in toxicity of 4-MBC during the UV/persulfate process.

v. To evaluate the performance of the UV/persulfate process on 4-MBC degradation in a swimming pool.

doi:10.6342/NTU201901036

Chapter 2 Literature review

2.1 4-Methylbenzylidene camphor

4-Methylbenzylidene camphor (4-MBC) is one of the most widely and frequently used organic UV filters and is classified as an UVB filter since its absorption peak is at 300 nm.

Table 2 lists the physicochemical properties of 4-MBC. In addition to commercial 4-MBC which occurs only as (E)-4-MBC, 4-MBC undergoes reversible E–Z (trans–cis) isomerization after exposure to light [10, 25, 26].

Organic UV filters are included not only in sunscreens but also in many products in daily use, such as cosmetics, body lotions, hair sprays, hair dyes, shampoos and bubble baths, for product stability and durability. Nevertheless, growing concerns about the acute (sunburn) and chronic (skin cancer) effects of sunlight irradiation have led to the increasing usage of sunscreens. The concentration limits of 4-MBC that can be added in sunscreen formulations range from 4% to 6% of the product weight, depending on the different regulations worldwide [27].

Organic UV filters can enter the aquatic environment through two major pathways. One pathway is direct discharge via recreational activities (e.g., swimming), and the other is indirect input via wastewater treatment plants (WWTPs). However, organic UV filters

doi:10.6342/NTU201901036

cannot be efficiently degraded in conventional WWTPs. The effluents containing these compounds discharge into rivers and seas and accumulate in other matrices. Therefore, 4-MBC has been detected in different aqueous matrices, such as bathing waters, swimming pool waters, tap waters, wastewaters, surface waters, and seawater, and even in sludge, marine sediments, beach sand, river sediments and fish lipids, as shown in

Table 3.

Moreover, due to its high lipophilicity (Log K_{ow} of 4.95) and nonbiodegradable characteristics, 4-MBC has the potential for bioaccumulation in the environment and is concentrated in living organisms [3, 4, 28]. Several previous studies have reported that 4-MBC was detected in plasma, urine, and human milk [29, 30]. In addition, 4-MBC was identified as the UV filter showing estrogenic activity in *in vitro* and *in vivo* assays [31]. As mentioned in previous work [32, 33], 4-MBC not only decreases the litter size and survival rate of rats but also accelerates cell proliferation in human breast cancer cells. Furthermore, 4-MBC shows an inhibitory effect on neuronal and muscular development in zebrafish embryos [34]. Therefore, it is urgent and imperative to develop an effective degradation process for 4-MBC.

doi:10.6342/NTU201901036

Table 2. Physicochemical properties of 4-MBC.

Compound	Abbreviation	Structure
4-Methylbenzylidene camphor	4-MBC	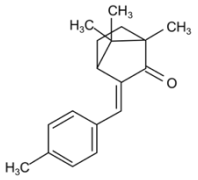
Molecular mass (g/mole)	**Log K_{ow}**	
254.37	4.95	
Solubility (g/L)	**λ (nm)**	
5.1×10^{-3}	300	

Table 3. Detected concentrations of 4-MBC in water, sediments, beach sand and sludge samples.

Sample	Concentration	Location	Reference
Bathing waters	n.a–21 ng L^{-1}	Greece	[35]
Swimming pool waters	n.a–7.9 ng L^{-1}	Greece	[5]
	n.a–300 ng L^{-1}	Slovenian	[6]
Tap water	n.a–58 ng L^{-1}	Spain	[7]
Groundwater	n.a–13.9 ng L^{-1}	Spain	[8]
Wastewaters (influent)	n.a–6.5 μg L^{-1}	Switzerland	[3, 4]
Wastewaters (effluent)	n.a–2.7 μg L^{-1}	Switzerland	[3, 4]
	321–11,700 ng L^{-1}	Antarctic	[9]
Surface waters	n.a–28 μg L^{-1}	Switzerland	[3, 4]
	n.a–82 ng L^{-1}	Switzerland	[10]
	n.a–642 ng L^{-1}	Melbourne	[11]
	n.a–379 ng L^{-1}	Hong Kong	[12]
Seawater	n.a–798.7 ng L^{-1}	Norway	[13]
	n.a–45.1 ng L^{-1}	Antarctic	[9]
	n.a–1043.4 ng L^{-1}	Spain	[14]
Sewage sludge	150–4980 μg kg^{-1} (d.m.)*	Switzerland	[25]
Marine sediments	n.a–7.90 ng g^{-1} (d.m.)*	Colombia	[36]
	n.a–31.3 ng g^{-1}	China	[37]

doi:10.6342/NTU201901036

Beach sand	n.a–2.4 ng g^{-1}	Spain	[38]
River sediments	n.a–17.2 ng g^{-1} (d.m.)*	Colombia	[36]
	n.a–1.2µg kg^{-1} (d.m.)*	Melbourne	[11]
	n.a–3.68 ng g^{-1}	China	[37]
Fish Lipids (***Perca fluviatilis***)	n.a–166 ng g^{-1}	Switzerland	[3, 4]
Fish Lipids (***Coregonus sp.roach***) (***Rutilus rutilus***)	50–1800 ng g^{-1}	Switzerland	[28]

* dry matter [d.m.]

doi:10.6342/NTU201901036

2.2 UV/persulfate process

Persulfate can be found in the form of three salts, i.e., sodium, potassium and ammonium persulfate. However, as Table 4 shows [39], potassium persulfate has very low solubility, and ammonium persulfate is unstable due to the oxidation of the ammonium ion and of ammonia by persulfate [39]. Therefore, sodium persulfate is the first choice for chemical oxidation treatment.

Table 4. Formula and solubility of three persulfate salts.

	Sodium persulfate	Potassium persulfate	Ammonium persulfate
Formula	$Na_2S_2O_8$	$K_2S_2O_8$	$(NH_4)_2S_2O_8$
Solubility (g/100g of H_20)	73	6	85

Sodium persulfate ($Na_2S_2O_8$), with a redox potential of 2.01 V, is the most commonly used persulfate salt for chemical oxidation treatment. However, the direct reactions of persulfate with organic contaminants are slow. To reach a satisfactory degradation rate, activation to generate reactive radical species such as SO_4^{-}• and HO• is needed.

Persulfate can be activated by energy (ultraviolet (UV), heat, ultrasound, radiolysis, etc.) or a catalyst (transition metals) to produce SO_4^{-}•. Among these activation methods, UV is considered the most easily operated and efficient method. According to the wavelength distribution [40], persulfate absorption ranges from the deep-UV region to 350 nm. All UV light sources (UVA, UVB, UVC, etc.) are capable of activating persulfate.

doi:10.6342/NTU201901036

In particular, UVC irradiation, which is widely used for drinking water disinfection, is regarded as the most efficient light source to activate persulfate. Two sulfate radicals are formed by the cleavage of peroxide bonds as UV gives energy to persulfate (Eq. 3) [41].

$$S_2O_8^{2-} + hv \rightarrow 2SO_4^- \bullet \qquad \text{Eq. 3}$$

$SO_4^{-}\bullet$ is a strong one-electron oxidant with a high redox potential (2.5−3.1 V) and is selective and applicable in a wide pH range. $SO_4^{-}\bullet$ reacts with water to generate HO•, which is the dominant radical in basic conditions (Eq. 4-5) [42]. After electron-transfer oxidations, $SO_4^{-}\bullet$ is transformed to sulfate anion (SO_4^{2-}), which does not require any particular disposal method and poses unreasonable risk.

$$SO_4^- \bullet + H_2O \rightarrow SO_4^{2-} + HO \bullet + H^+ \qquad k < 60\ M^{-1}s^{-1} \qquad \text{Eq. 4}$$

$$SO_4^- \bullet + OH^- \rightarrow SO_4^{2-} + HO \bullet \qquad k = 6.5 \pm 1.0 \times 10^7 M^{-1}s^{-1} \qquad \text{Eq. 5}$$

Sulfate radical-based processes are promising treatments for efficiently removing recalcitrant organics since sulfate radical is more selective for oxidation through electron-transfer reactions. One study investigated the degradation of 59 volatile organic compounds (VOCs) in a thermally activated persulfate process, indicating that organic contaminants with carbon-carbon double bonds or with benzene rings bonded to reactive functional groups are easily degraded through this process [43].

UV/persulfate has been successfully utilized in the laboratory studies to eliminate a variety of emerging contaminants, such as PPCPs, endocrine-disrupting chemicals,

doi:10.6342/NTU201901036

persistent organic pollutants, and disinfection byproducts, as shown in Table 5. As presented in Table 5, the target compounds, except for perfluorooctanoic acid (PFOA), can be almost completely decomposed within one and a half hours, with the molar ratio of persulfate to target compound ranging from six to one hundred.

doi:10.6342/NTU201901036

Table 5. Degradation of emerging contaminants using UVC/persulfate process.

Category	Compound	Concentration (Compound & Persulfate)	Reaction time	Removal (%)	Reference
PPCPs	Sulfamethazine	$[SMT]_0$= 0.02 mM $[Persulfate]_0$= 0.2 mM	45 min	96.5%	[44]
	Chloramphenicol	$[CAP]_0$= 31 μM $[Persulfate]_0$= 0.25 mM	40 min	100%	[45]
EDCs	Methyl paraben	$[MP]_0$= 32.8 μM $[Persulfate]_0$= 1 mM	90 min	98.9%	[46]
	2,4-Di-tert-butylphenol	$[2,4\text{-}D]_0$= 24.2 μM $[Persulfate]_0$= 1 mM	30 min	85.6%	[47]
POPs	PFOA	$[PFOA]_0$= 150 μM $[Persulfate]_0$= 15 mM	8 hr	83%	[48]
	Endosulfan	$[Endosulfan]_0$= 2.45 μM $[Persulfate]_0$= 24.5 μM	80 min	85%	[49]
DBPs	Butylated Hydroxyanisole	$[BHA]_0$= 0.3 mM $[Persulfate]_0$= 2 mM	20 min	100%	[50]
	Haloacetonitriles	$[HANs]_0$= 2 μM $[Persulfate]_0$= 200 μM	20 min	100%	[51]

doi:10.6342/NTU201901036

Chapter 3 Materials and Methods

3.1 Chemicals and standards

The formic acid (ACS grade) and methanol (HPLC-MS grade) were purchased from Riedel-deHaën (Seelze, Germany). Methanol (HPLC grade) was obtained from Mallinckrodt Baker (Phillipsburg,PA, USA). 4-Methylbenzylidene camphor (4-MBC), sodium persulfate, hydrogen peroxide, *tert*-butanol, sodium hydroxide, hydrochloric acid and humic acid were purchased from Sigma-Aldrich (St. Louis, MO, USA). Benzoic acid, sodium chloride and sodium sulfate were obtained from J.T. Baker (Philipsburg, NJ, USA). Phosphoric acid, dipotassium hydrogen phosphate and potassium dihydrogen phosphate were obtained from Nacalai Tesque (Kyoto, Japan). All of the chemicals were of analytical reagent grade and were used as received without further purification. 4-MBC stock solution was prepared in methanol and stored at –20 ℃. Other solutions were prepared in deionized (DI) water and stored at 4 ℃.

The outdoor swimming pool water for simulating the degradation of 4-MBC in real water matrix was collected in March 2019 from the outdoor swimming pool of National Taiwan university. The water sample was filtered through 0.22 μm glass fiber membrane and stored at 4 ℃ prior to using.

doi:10.6342/NTU201901036

3.2 Experimental procedures

The typical reaction experiment was performed in a 25 mL quartz tube containing 4-MBC (0.39 μM) and persulfate (42 μM). Solution pH was adjusted to a desirable value with 0.1 M HCl and 0.1 M NaOH. The solution was irradiated with monochromatic light (254 nm) from a low-pressure mercury lamp (8W, Sankyo, Japan), which was initially warmed for 30 min to reach constant output. All experiments were conducted at room temperature (25 ± 1 ℃). At designated time intervals, 1 mL aliquots were withdrawn. After that, the sample vials were kept in a 4 ℃ refrigerator for further analysis. All kinetic experiments were performed in triplicate, and the error bars represent the standard deviations among triplicate.

3.3 Determination of second-order rate constant

Second-order rate constant for reaction of SO_4^{-}• with 4-MBC was estimated by competition kinetic method using benzoic acid (BA) as a reference compound. Experiments were carried out in a 25 mL quartz tube containing 4-MBC (3.9 μM), BA (3.9 μM) and persulfate (420 μM). 4.2 mM *tert*-butanol (TBA) was spiked into the solution to quench HO• during the UV/persulfate process. 1 mL aliquots were withdrawn from the quartz tube at designated time intervals, and kept in a 4 ℃ refrigerator for further analysis.

doi:10.6342/NTU201901036

3.4 Analytical methods

4-MBC was quantified by a high-performance liquid chromatography with a tandem mass spectrometer (Sciex API 4000 HPLC-MS/MS) with an electro-spray ionization (ESI) interface. Chromatographic separations were performed using a ZORBAX Eclipse XDB-C_{18} column (150 × 4.6 mm, 5μm). Analyses were performed in positive mode. The gradient mobile phase consisted of 0.1% (v/v) formic acid in DI water/0.1% (v/v) formic acid in methanol (HPLC grade) (A/B) at a flow rate of 0.9 mL/min, which started with 95/5 for 0.5 min, and increased linearly from 95/5 to 5/95 for the next 1 min and kept for 3.5 min. Then returned to 95/5 in 0.5 min, and held for 2 min. The sample injection volume was 20 μL. The commercial 4-MBC mainly (>99%) consist of the (E)-4-MBC. Therefore, the determinations of (E)- and (Z)-4-MBC were all using the calibration curve of (E)-4-MBC, assuming the same detector response for respective (E)- and (Z)-4-MBC. As Figure S2 shown, the retention time of (E)-4-MBC and (E)-4-MBC are 5.64 and 5.82 minutes, respectively. If not otherwise noted, 4-MBC data were summed and reported as totals. The quantitation of 4-MBC was performed using m/z of 255 for precursor ion and 105 for product ion. The confirmation of 4-MBC was performed using m/z of 255 for precursor ion and 171 for product ion.

Benzoic acid was detected by high-performance liquid chromatography with diode-array detection (HPLC-DAD). The spectrophotometer was an Agilent 1200 module

doi:10.6342/NTU201901036

equipped with a ZORBAX Eclipse XDB-C_{18} column (150 × 4.6 mm, 5μm). The mobile phase was a mixture of methanol and 10.0 mM phosphoric acid (50:50, v/v) at a flow rate of 1.0 mL min^{-1}. The sample injection volume was 100 μL and the detection wavelength was 227 nm.

Sulfate was measured by an ion chromatography system (Metrohm 790 Personal IC). The mobile phase was a mixture of 1 mM sodium hydrogen carbonate and 3.2 mM sodium carbonate. Chromatographic separations were performed using a Metrosep A Supp 5 column (250 × 4.0 mm, 5μm).

3.5 Product identification

The transformation products generated during UV/persulfate process were analyzed by an AB SCIEX Triple TOF™ 5600 operated in ESI mode. Chromatographic separations were performed using a ZORBAX Eclipse XDB-C_{18} column (150 × 4.6 mm, 5μm). Accurate MS and MS/MS patterns of 4-MBC and its transformation products were analyzed in a molecular ion scanning mode (m/z 50 to 400) in positive mode. The gradient mobile phase consisted of 0.1% (v/v) formic acid in DI water/0.1% (v/v) formic acid in methanol (HPLC-MS grade) (A/B) at a flow rate of 0.9 mL/min, which started with 95/5 for 0.5 min, and changed linearly from 95/5 to 5/95 for the next 1 min and kept for 3.5 min. Then returned to 95/5 in 0.5 min, and held for 2 min. The sample injection volume

doi:10.6342/NTU201901036

was 50 μL.

3.6 Microtox® acute toxicity test

The change in the acute toxicity during UV/persulfate degradation of 4-MBC was carried out by measuring the decrease in the bioluminescence of *Vibrio fischeri* with a Microtox® Model 500 Analyzer (Microbics Corp., Carlsbad, CA, USA). Before toxicity tests, the pH values of all samples were adjusted to 7 to avoid affecting toxicity. Samples were tested containing 2% sodium chloride, in five dilutions. The change of luminescence was recorded after 5 and 15 min, compared to that of toxic-free control. EC_{50} (the concentration causing 50% *Vibrio fischeri* death) values are expressed as a percentage (% v/v) of the initial sample. The final toxicity value is expressed in toxicity units (TU; TU = $100/EC_{50}$).

doi:10.6342/NTU201901036

Chapter 4 Results and Discussion

4.1 Comparison of 4-MBC degradation by direct UV photolysis, persulfate dark oxidation and the UV/persulfate process

Initial experiments were carried out to determine the 4-MBC degradation efficiency under the three different conditions, including UV irradiation, persulfate dark oxidation and the UV-activated persulfate process (UV/persulfate), as shown in Figure 1. There was no appreciable direct UV photolysis of 4-MBC; 4-MBC was also stable in the presence of persulfate (42 μM) alone in the dark. However, the combination of UV irradiation and persulfate significantly enhanced the degradation of 4-MBC. Under the conditions of $[4\text{-MBC}]_0$ = 0.39 μM, $[\text{persulfate}]_0$ = 42 μM and initial pH = 7, up to 90% of 4-MBC was destroyed within 6 min. The improved degradation efficiency of 4-MBC indicated a synergistic effect in the UV/persulfate process. Considering that no measurable degradation of 4-MBC was observed for either direct UV photolysis or persulfate dark oxidation, 4-MBC degradation in the UV/persulfate process could be attributed to the generation of reactive radicals, such as SO_4^{-}• and HO• [41].

4-MBC comprises geometrical (E)- and (Z)-isomers. As shown in Figure 2, under UV irradiation alone, (E)-4-MBC was found to partially transform into (Z)-4-MBC, and both isomers were stable throughout the reaction time. Previous studies have also

doi:10.6342/NTU201901036

observed the same phenomenon, in which 4-MBC experienced rapid photoisomerization and achieved equilibrium within minutes [10, 25, 26]. However, in the UV/persulfate process, 4-MBC not only experienced photoisomerization between (E)- and (Z)-4-MBC but was also simultaneously degraded; within 6 min, more than 90% of all 4-MBC was decomposed. In the following text, the concentrations of (E)- and (Z)-4-MBC, have been summed and reported as totals if not otherwise mentioned.

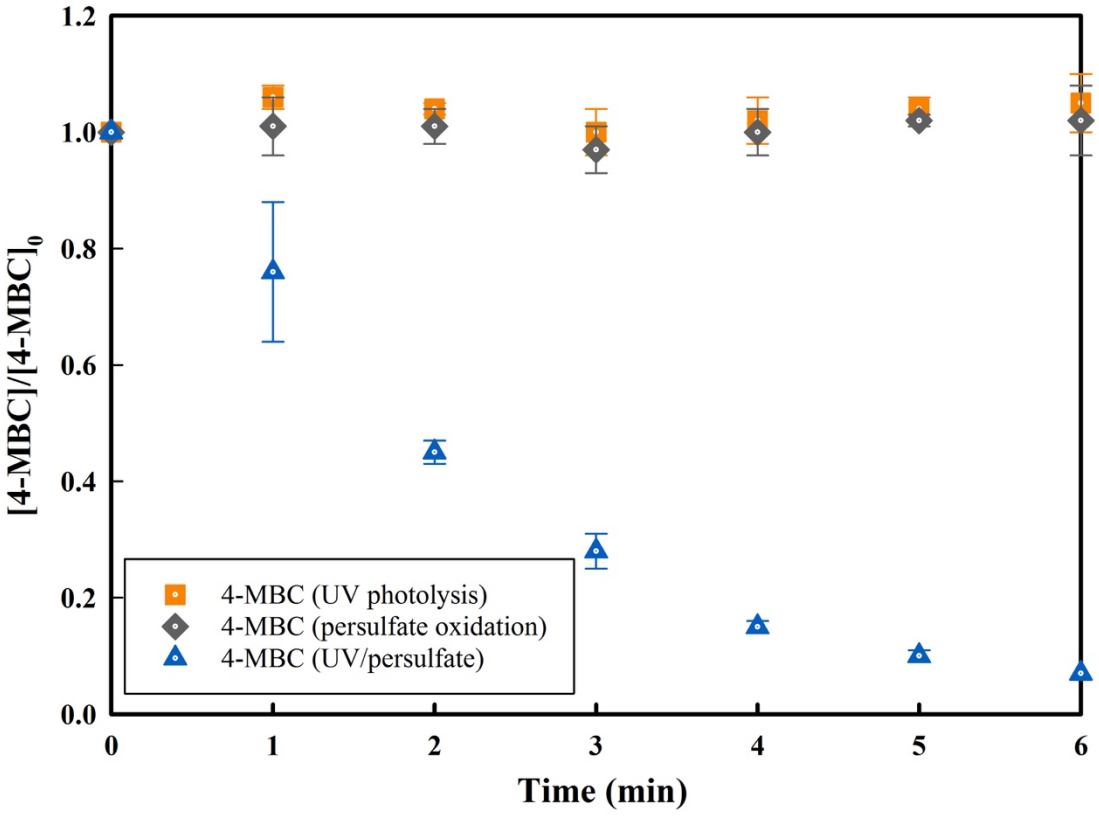

Figure 1. Degradation of 4-MBC under direct UV photolysis, persulfate dark oxidation and the UV/persulfate process. Experimental conditions: $[4\text{-MBC}]_0$ = 0.39 μM, $[\text{persulfate}]_0$ = 42 μM, initial pH = 7, reaction time = 6 min.

doi:10.6342/NTU201901036

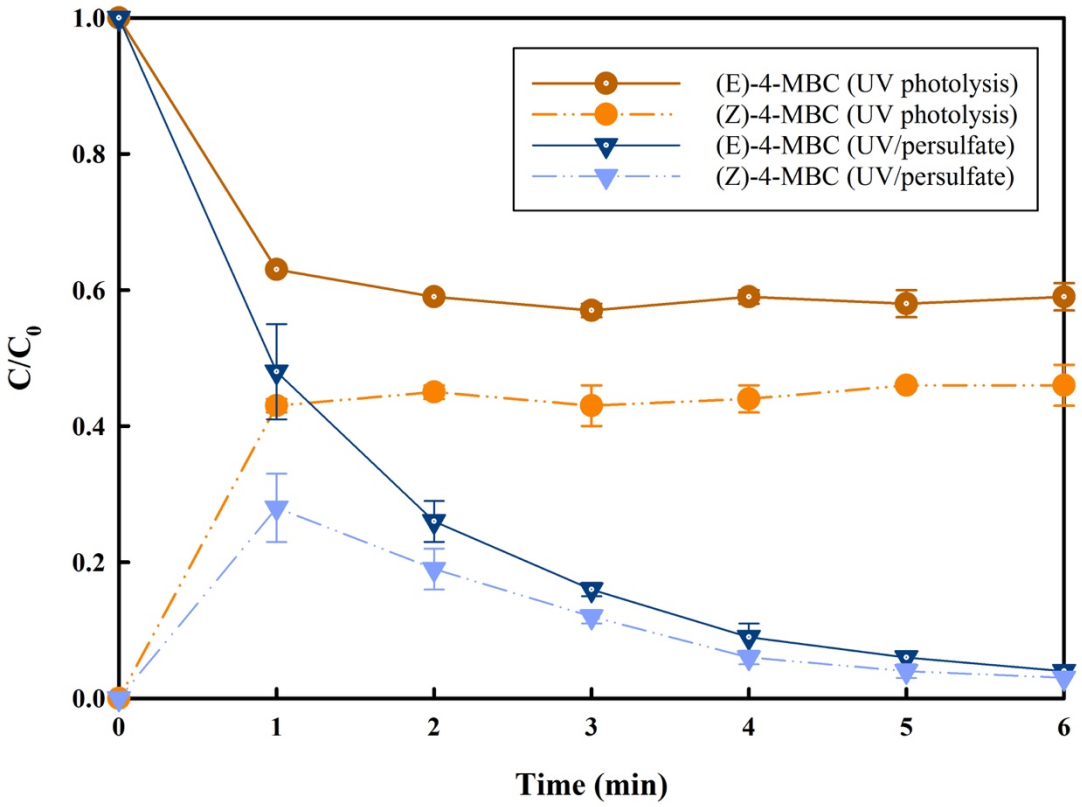

Figure 2. Degradation of (E)-4-MBC and (Z)-4-MBC under direct UV photolysis and the UV/persulfate process. Experimental conditions: $[4\text{-MBC}]_0$ = 0.39 μM, $[\text{persulfate}]_0$ = 42 μM, initial pH = 7, reaction time = 6 min.

doi:10.6342/NTU201901036

4.2 Effect of initial persulfate dosage

The dosage of persulfate, which serves as a source of reactive radicals (e.g., HO• and SO_4^{-}•), is an important operation parameter in the UV/persulfate process. The effect of the initial persulfate dosage on 4-MBC degradation was studied in the range of 4.2 μM to 42 μM at an initial pH of 7.0. A pseudo-first-order kinetics model was utilized to describe 4-MBC degradation under the UV/persulfate process (Eq. 6),

$$\ln\left(\frac{[4-MBC]}{[4-MBC]_0}\right) = -k_{obs}t \qquad \text{Eq. 6}$$

where $[4\text{-MBC}]_0$ is the initial concentration (μM) of 4-MBC; [4-MBC] is the concentration of 4-MBC at time t (min); and k_{obs} is the pseudo-first-order rate constant (min^{-1}).

Figure 3 shows that 4-MBC degradation exhibited pseudo-first-order kinetics at all persulfate dosages. Moreover, an increase in persulfate dosage indeed resulted in a significant improvement in k_{obs}, as shown in Figure 4. k_{obs} increased from 4.0×10^{-2} to 44.8×10^{-2} min^{-1} as the persulfate dosage increased from 4.2 μM to 42 μM. Figure 4 also demonstrates a linear relationship between k_{obs} and persulfate dosage ($k_{obs} = 0.0464 \times$ [persulfate] − 0.0153, $R^2 = 0.997$). The acceleration of 4-MBC degradation with higher persulfate dosage could be attributed to the increase in reactive radicals in the presence of a higher persulfate dosage. A similar trend has been reported for methyl paraben and chloramphenicol degradation at various persulfate dosages in the UV/persulfate process

doi:10.6342/NTU201901036

[45, 46]. Nevertheless, several previous studies have investigated perfluorocarboxylic acid degradation in the UV/persulfate process and reported that an increase in the initial persulfate dosage could not always accelerate the pollutant degradation rate [40, 48] because of the self-scavenging behavior of SO_4^-•, as shown in Eq. 7 [52]. However, this self-scavenging effect was not observed in this study, probably because the highest persulfate dosage used in this work (42 μM) did not reach the critical level that started to hinder 4-MBC degradation.

$$SO_4^- \bullet + SO_4^- \bullet \rightarrow S_2O_8^{2-} \qquad \text{Eq. 7}$$

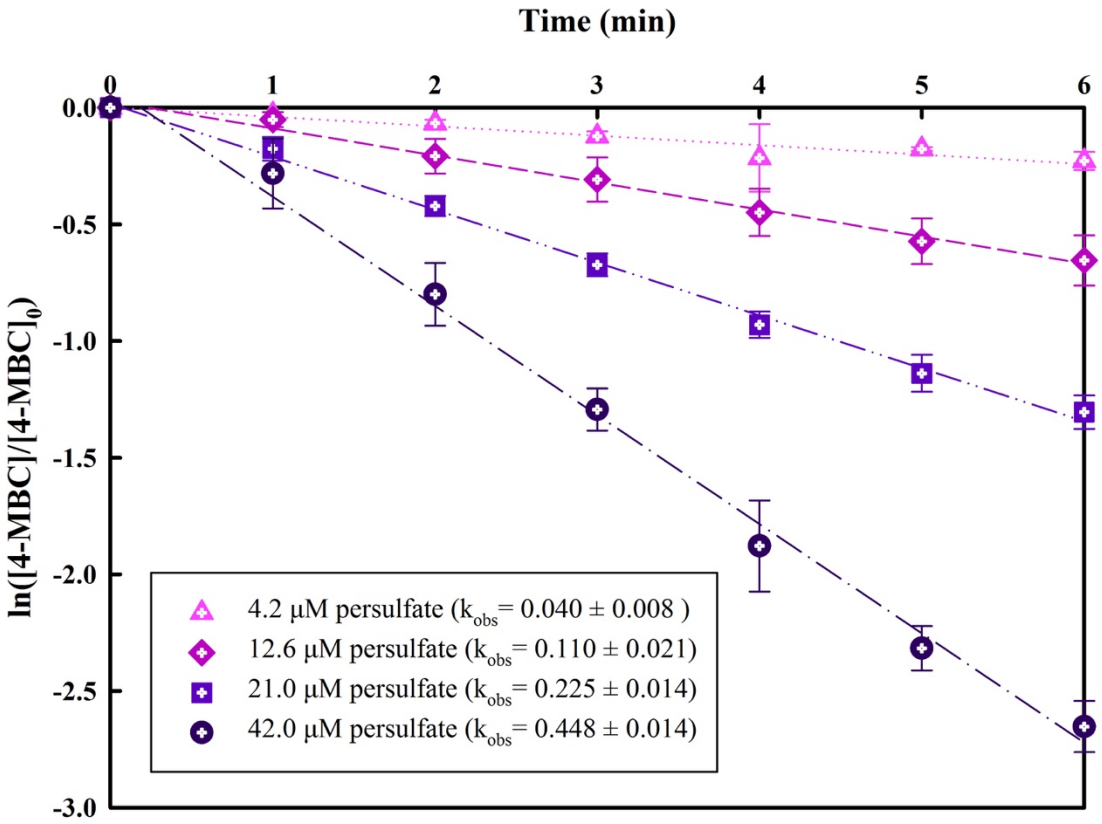

Figure 3. Effect of persulfate dosage on 4-MBC degradation in the UV/persulfate process. Experimental conditions: $[4\text{-MBC}]_0$ = 0.39 μM, $[\text{persulfate}]_0$ = 4.2–42 μM, initial pH = 7, reaction time = 6 min.

doi:10.6342/NTU201901036

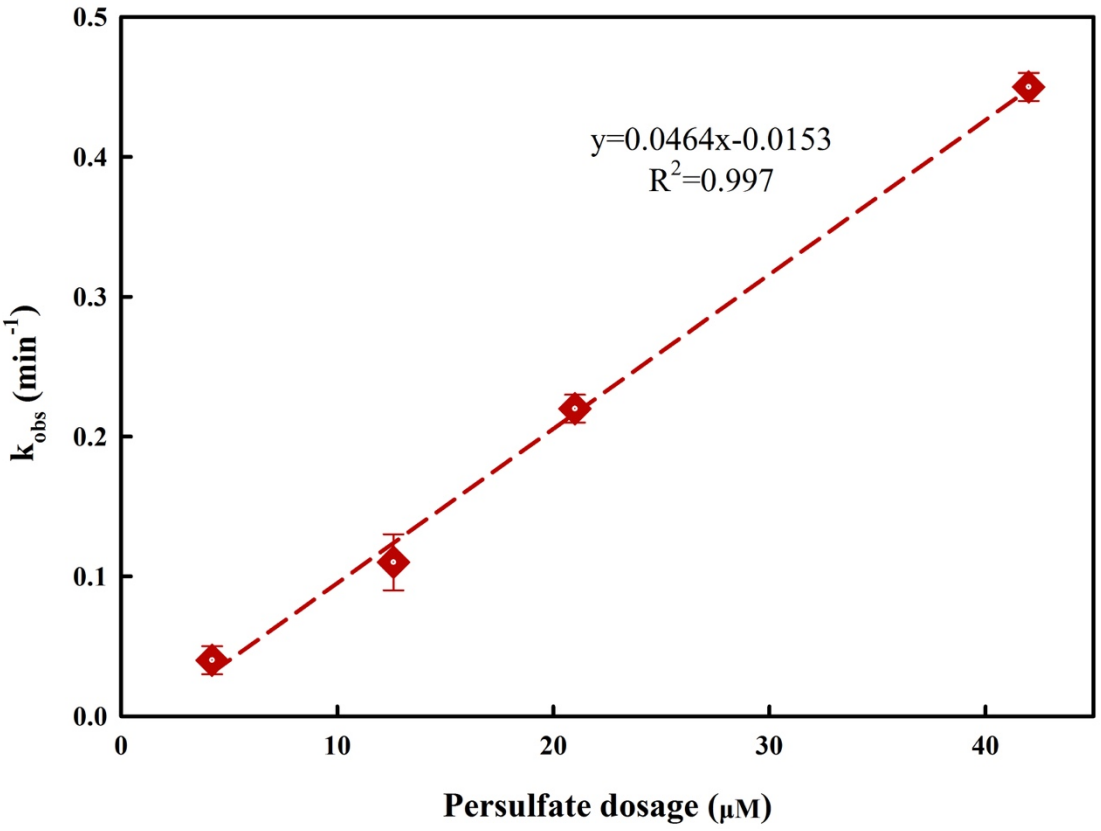

Figure 4. A linear relationship between k_{obs} and persulfate dosage in the UV/persulfate process. Experimental conditions: $[4\text{-MBC}]_0$ = 0.39 μM, $[\text{persulfate}]_0$ = 4.2−42 μM, initial pH = 7.

doi:10.6342/NTU201901036

4.3 Effect of solution pH

The solution pH, which affects radical generation (Eq. 8-9) [53], is also an important factor in evaluating the efficiency of the UV/persulfate process. Considering the fact that the quantum efficiency of photodissociation and the molar extinction coefficient of persulfate at a 254 nm wavelength are identical at different pH values [52]; the different degradation rates that occurred at various pH values could be mainly ascribed to the different radicals (e.g., HO• and SO_4^-•) dominating 4-MBC degradation.

$$SO_4^- \bullet + OH^- \rightarrow SO_4^{2-} + HO \bullet \qquad \text{Eq. 8}$$

$$SO_4^- \bullet + H_2O \rightarrow H^+ + SO_4^{2-} + HO \bullet \qquad \text{Eq. 9}$$

Prior to the investigation of the effect of solution pH on 4-MBC degradation, background experiments were conducted to ensure the reasonableness of the data. First, the effect of the presence of phosphate buffer was studied, as shown in Figure 5. Phosphate buffer was utilized to maintain the solution pH during the UV/persulfate process. We found that regardless of whether 1 mM or 5 mM phosphate buffer was added, the degradation of 4-MBC was seriously inhibited. Similar results have also been reported, in which phosphate buffer inhibits the reactivity of SO_4^-• and HO• [46, 54, 55]. Second, Table 6 lists the final pH under different initial persulfate dosages without using the phosphate buffer during the UV/persulfate process. The solution pH dropped from 7.0 to 4.9 with increased persulfate dosage (i.e., from 4.2 μM to 42 μM), where the higher the

doi:10.6342/NTU201901036

persulfate dosage used was, the more the pH dropped. This phenomenon has also been observed in several previous studies [45, 48, 50]. Acidic byproduct generation during persulfate decomposition may be the major rationale for the pH decrease during the UV/persulfate process; such reaction include the formation of 1) acidic degradation byproducts and 2) acidic photoproducts of persulfate, such as bisulfate (HSO_4^-) and protons (H^+) (Eq. 10-13), as well as 3) acidic inorganic products, such as peroxysulfuric acid (H_2SO_5) and sulfuric acid (H_2SO_4) (Eq. 14-15). Consequently, to avoid the phosphate buffer effect and to maintain the pH during the reaction (within an allowance of plus or minus 0.5), as well as to observe the 4-MBC degradation phenomenon via the UV/persulfate process, phosphate buffer was not used. Additionally, a spiked persulfate dosage of 12.6 μM was determined for use in subsequent experiments.

$$S_2O_8^{2-} + H_2O \rightarrow 2HSO_4^- + 0.5O_2 \quad \text{Eq. 10}$$

$$S_2O_8^{2-} + H^+ \rightarrow HS_2O_8^- \quad \text{Eq. 11}$$

$$HS_2O_8^- \rightarrow SO_4 + HSO_4^- \quad \text{Eq. 12}$$

$$HSO_4^- \rightarrow H^+ + SO_4^{2-} \quad \text{Eq. 13}$$

$$HS_2O_8^- + H_2O \rightarrow H_2SO_5 + HSO_4^- \quad \text{Eq. 14}$$

$$H_2SO_5 + H_2O \rightarrow H_2O_2 + H_2SO_4 \quad \text{Eq. 15}$$

To determine the effect of solution pH, 4-MBC degradation experiments were carried out at pH values ranging from 5 to 9 (Figure 6). k_{obs} remained approximately

doi:10.6342/NTU201901036

constant from 11.8 × 10^{-2} min^{-1} to 11.0 × 10^{-2} min^{-1} in acidic and neutral solutions and then significantly decreased to 6.8 × 10^{-2} min^{-1} in basic conditions. A previous study also reported that an increase in solution pH resulted in a decrease in the degradation rate of the antineoplastic drug azathioprine in the UV/persulfate process [56]. Based on Eq. 8, with further increases in solution pH, the increased OH^- in the solution tends to react with SO_4^{-}• and further produce HO•, which gradually replaces SO_4^{-}• as the dominant radical. Thus, it is supposed that SO_4^{-}• is the predominant reactive species for 4-MBC degradation; additionally, compared to HO•, SO_4^{-}• likely exhibits a much greater reactivity towards 4-MBC, leading to the apparent rise in 4-MBC degradation efficiency under acidic and neutral conditions. Further verification of this assumption is discussed in the section 4.4.

Table 6. The final pH under different initial persulfate dosages.

$[Persulfate]_0$	**4.2 μM**	**12.6 μM**	**21.0 μM**	**42.0 μM**
Initial pH	**7.0**			
Final pH	**7.0**	**6.6**	**5.8**	**4.9**

doi:10.6342/NTU201901036

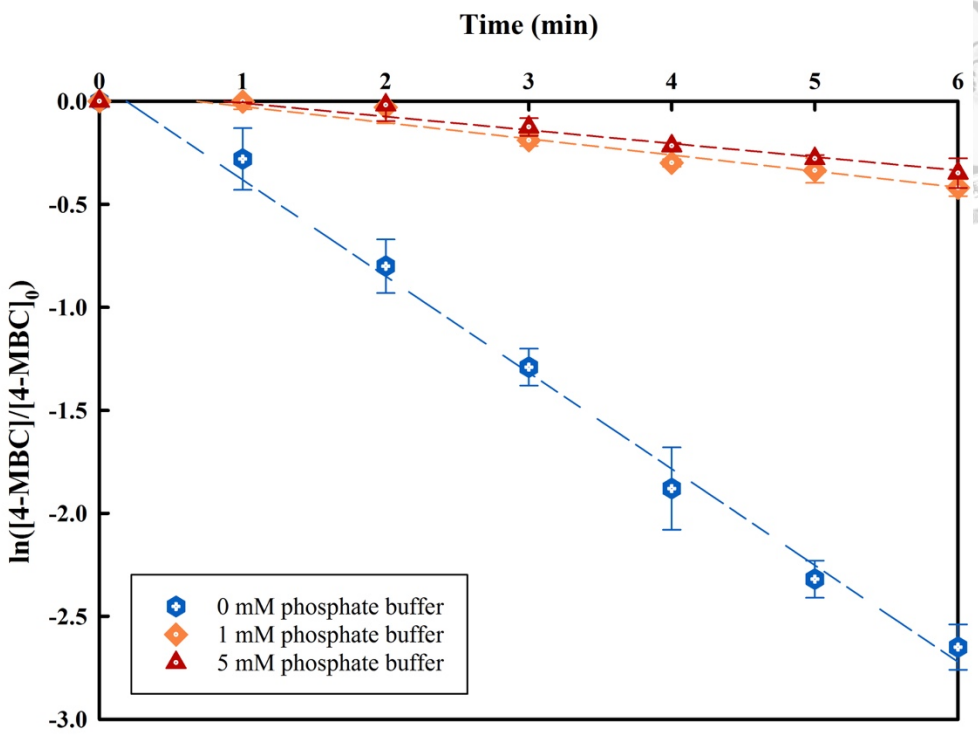

Figure 5. Effect of phosphate buffer on 4-MBC degradation in the UV/persulfate process. Experimental conditions: $[4\text{-MBC}]_0 = 0.39$ μM, $[\text{persulfate}]_0 = 42$ μM, [phosphate buffer] = 0 mM–5 mM, initial pH = 7, reaction time = 6 min.

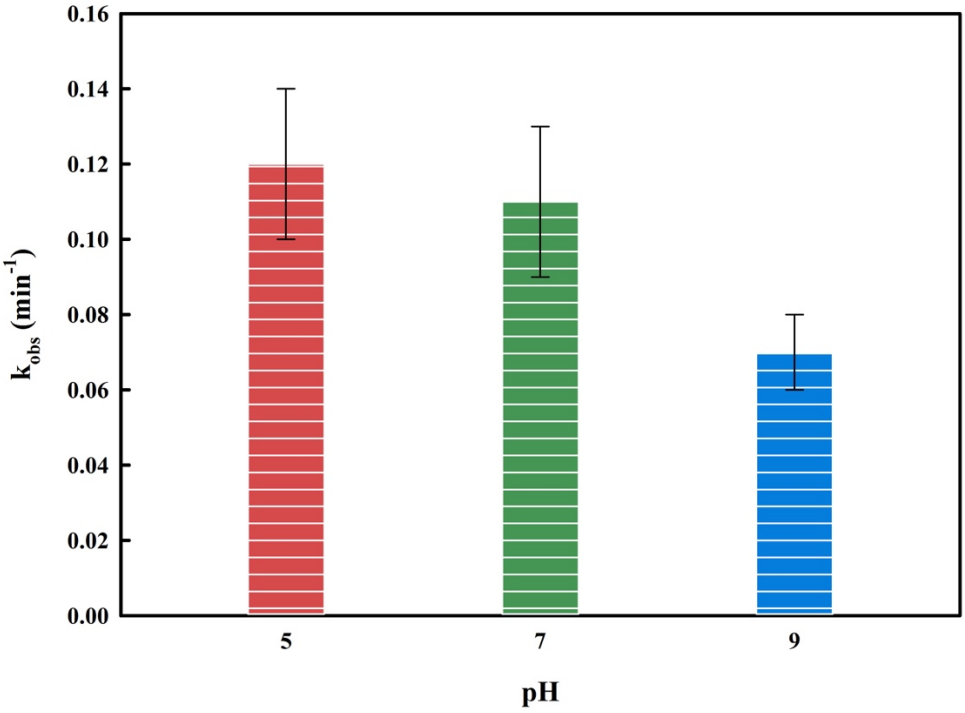

Figure 6. Effect of initial solution pH on 4-MBC degradation in the UV/persulfate process. Experimental conditions: $[4\text{-MBC}]_0 = 0.39$ μM, $[\text{persulfate}]_0 = 12.6$ μM, initial pH= 5, 7 and 9.

doi:10.6342/NTU201901036

4.4 Identification of reactive species

Based on the results discussed in the previous sections, the excellent degradation efficiency of 4-MBC in the UV/persulfate process may be ascribed to reactive radical (SO_4^{-}• and HO•) oxidation. The generation of SO_4^{-}• and HO• in the UV/persulfate process follows these equations (Eq.16-17) [22].

$$S_2O_8^{2-} + hv \rightarrow 2SO_4^{-}\bullet \qquad \text{Eq. 16}$$

$$SO_4^{-}\bullet + OH^{-} \rightarrow SO_4^{2-} + HO\bullet \quad k = 6.5 \times 10^7\ M^{-1}s^{-1} \qquad \text{Eq. 17}$$

First, to ensure that the degradation of 4-MBC was initiated by reactive radical oxidation, methanol (MeOH), which contains α-hydrogen, was used to quench both SO_4^{-}• and HO• (Eq. 18-19) [21, 22]. As shown in Figure 7, the degradation of 4-MBC was extremely inhibited in the presence of MeOH. This result suggested that reactive radicals (e.g., HO• and SO_4^{-}•) contributed to 4-MBC degradation in the UV/persulfate process.

$$SO_4^{-}\bullet + MeOH \rightarrow products \quad k = 1.1 \times 10^7\ M^{-1}s^{-1} \qquad \text{Eq. 18}$$

$$HO\bullet + MeOH \rightarrow products \quad k = 9.7 \times 10^8\ M^{-1}s^{-1} \qquad \text{Eq. 19}$$

Second, to identify the contribution of HO• and SO_4^{-}• to 4-MBC degradation in the UV/persulfate process, *tert*-butanol (TBA), which lacks α-hydrogen, was used to quench HO• but not SO_4^{-}• since the rate constants between TBA and SO_4^{-}• are significantly lower than those between TBA and HO• (Eq. 20-21) [21, 22]. Figure 8 shows that in the presence of TBA, no recognizable differences were observed at all studied pH values (5,

doi:10.6342/NTU201901036

7 and 9) in the UV/persulfate process. This result suggested that SO_4^{-}• was the major reactive radical in the UV/persulfate process for reaction with 4-MBC. To further verify this conclusion, experiments with a UV-activated hydrogen peroxide process (UV/H_2O_2) were also conducted to confirm whether HO• is insignificant in 4-MBC degradation. In the UV/H_2O_2 process, HO• is the major reactive radical species that degrades 4-MBC. As shown in Figure 8, no degradation of 4-MBC was observed under the UV/H_2O_2 process, even when using much higher oxidant dosages (42 μM) and longer reaction times (30 min) than those in the UV/persulfate process at pH 5, 7 and 9. These results reiterate that SO_4^{-}• is the dominant species under the UV/persulfate process.

$$SO_4^{-} \bullet + TBA \rightarrow products \quad k = 4.0 \times 10^5\ M^{-1}s^{-1} \qquad \text{Eq. 20}$$

$$HO \bullet + TBA \rightarrow products. \quad k = 6.0 \times 10^8\ M^{-1}s^{-1} \qquad \text{Eq. 21}$$

To further explore the reactivity of SO_4^{-}• in 4-MBC degradation, the second-order rate constant of SO_4^{-}• with 4-MBC ($k_{SO_4^{-}\bullet,4-MBC}$) was estimated by the competition kinetics method [54]. Benzoic acid (BA) was chosen as the reference compound for $k_{SO_4^{-}\bullet,4-MBC}$ determination; the second-order rate constant of SO_4^{-}• with benzoic acid ($k_{SO_4^{-}\bullet,BA}$) is 1.2 × 10^9 M^{-1} s^{-1} [22]. Background tests showed no removal of 4-MBC and benzoic acid upon UV irradiation or in the presence of persulfate alone in the dark within 6 min (Figure S1). Thus, the influence of UV photolysis and dark persulfate oxidation could be neglected in calculations. TBA was added to the solution to quench

doi:10.6342/NTU201901036

HO• in the UV/persulfate process. Therefore, the degradation of 4-MBC and benzoic acid was assumed to mainly occur by SO_4^{-}•. The second-order rate constant of SO_4^{-}• with 4-MBC ($k_{SO_4^{-}\bullet,4-MBC}$) can be calculated by Eq. 22.

$$\ln\left(\frac{[4-MBC]_0}{[4-MBC]_t}\right) = \frac{k_{SO_4^{-}\bullet,4-MBC}}{k_{SO_4^{-}\bullet,benzoic\ acid}} \ln\left(\frac{[benzoic\ acid]_0}{[benzoic\ acid]_t}\right) \qquad \text{Eq. 22}$$

Then, a straight line with the slope $k_{SO_4^{-}\bullet,4-MBC}/k_{SO_4^{-}\bullet,\text{Benzoic acid}}$ and an intercept of zero could be plotted with $\ln([\text{4-MBC}]_0/[\text{4-MBC}]_t)$ as the y-axis and $\ln([\text{benzoic acid}]_0/[\text{benzoic acid}]_t)$ as the x-axis. Figure 9 shows that the reaction rate constant ratio between 4-MBC and benzoic acid with SO_4^{-}• was 2.455 ± 0.05. Thus, the second-order rate constant of SO_4^{-}• with 4-MBC was calculated to be $(2.95 \pm 0.05) \times 10^9\ M^{-1}\ s^{-1}$. This value is near the diffusion-controlled limit, indicating that 4-MBC is susceptible to attack by SO_4^{-}•. Several previous studies have also estimated that the second-order rate constants of SO_4^{-}• with other compounds (e.g., 2,4,6-trichloroanisole and sulfasalazine) are near the diffusion-controlled limit [54, 57].

doi:10.6342/NTU201901036

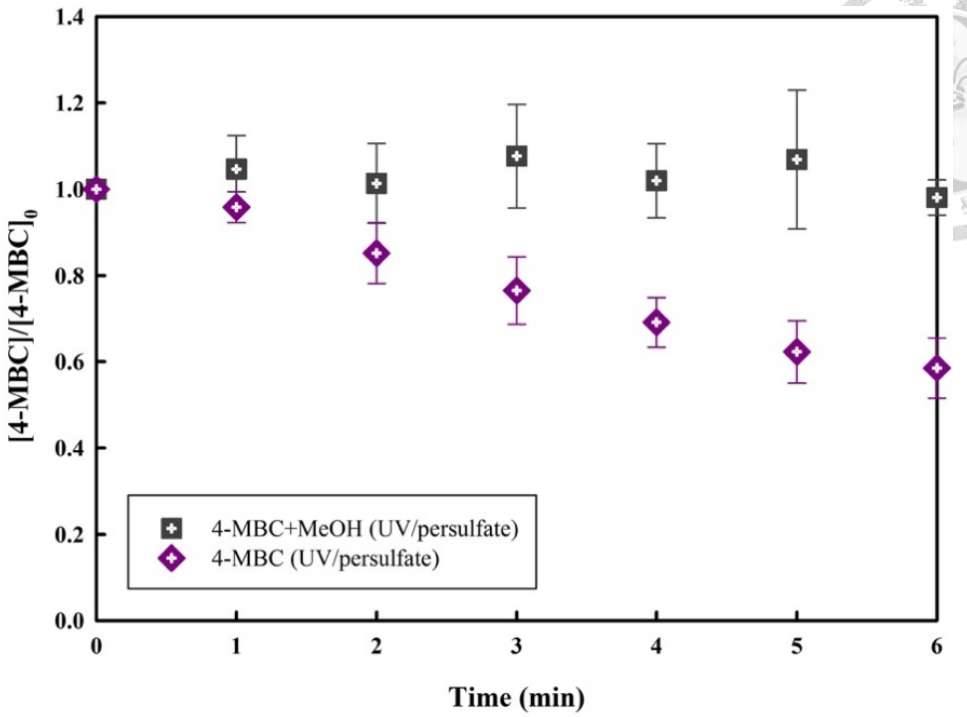

Figure 7. Effect of MeOH on the UV/persulfate process. Experimental conditions: [4-MBC]$_0$ = 0.39 μM, [persulfate]$_0$ = 12.6 μM, [MeOH] = 126 mM, initial pH = 7, reaction time = 6 min.

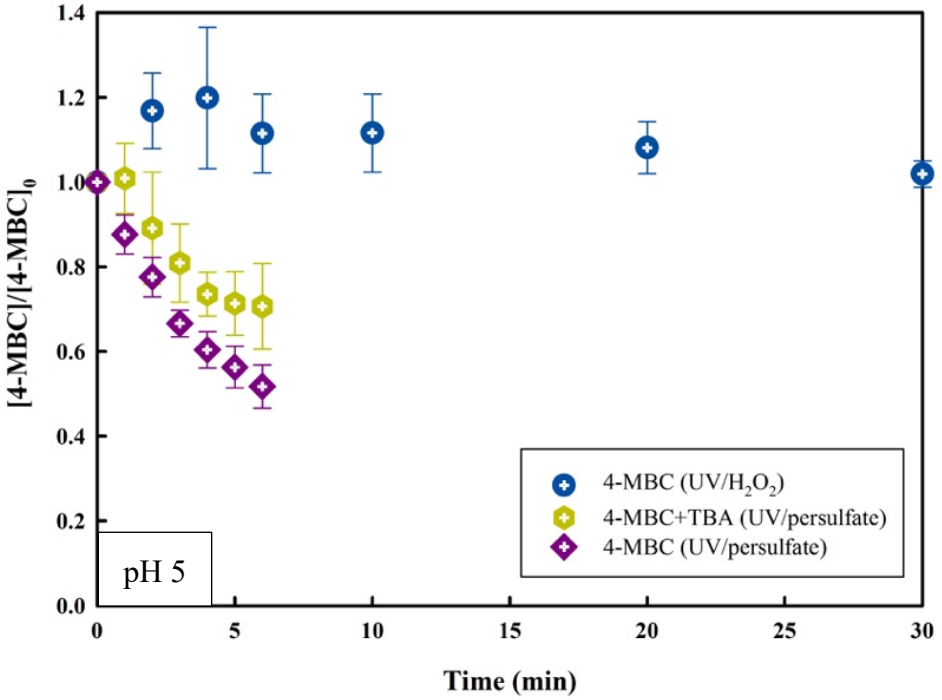

doi:10.6342/NTU201901036

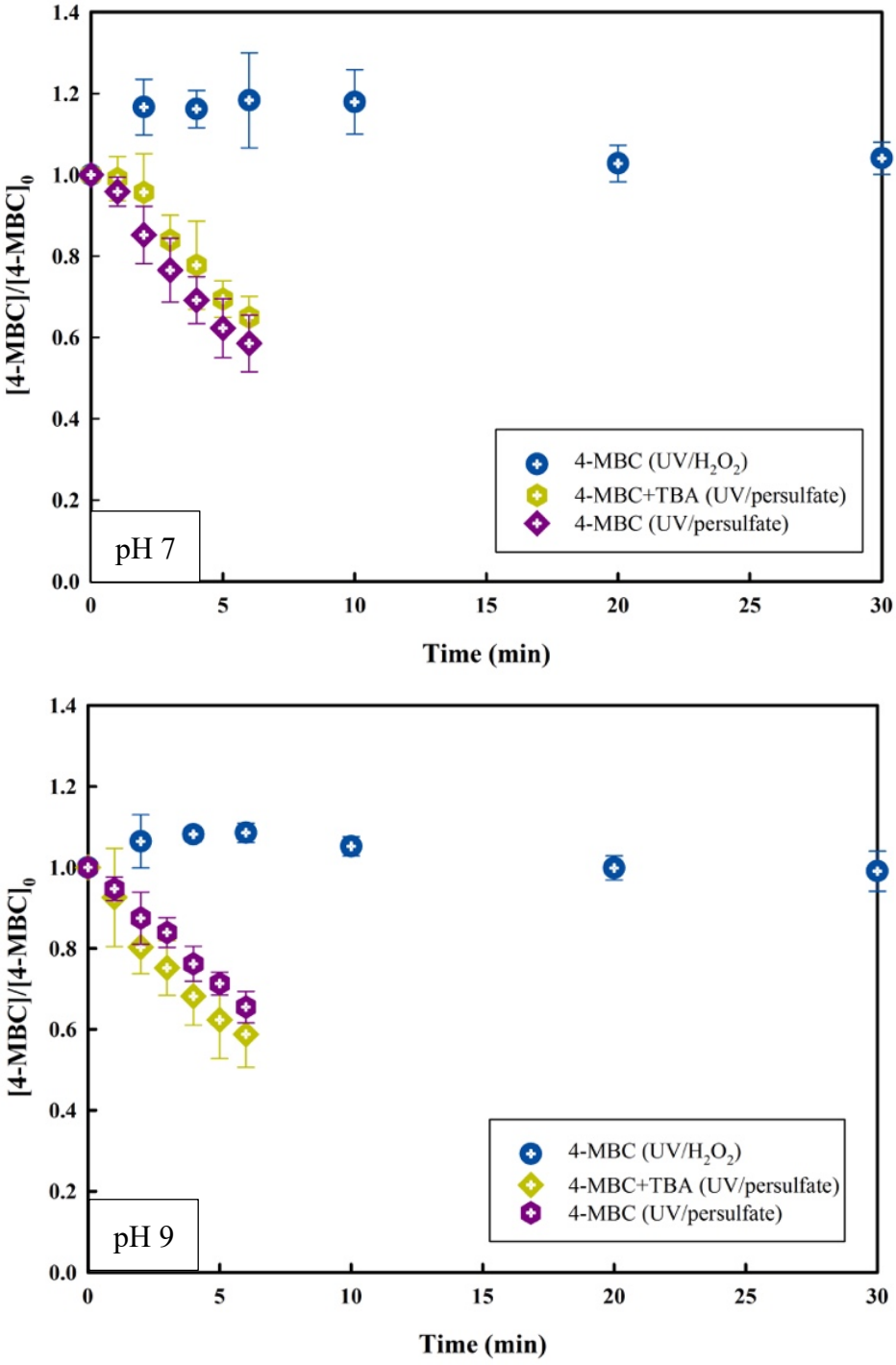

Figure 8. Effect of TBA on the UV/persulfate process and the degradation efficiency in the UV/H_2O_2 process at pH 5, 7 and 9. Experimental conditions: $[4\text{-MBC}]_0$ = 0.39 μM, $[\text{persulfate}]_0$ = 12.6 μM, $[\text{hydrogen peroxide}]_0$ = 42 μM, [TBA] = 1.26 mM.

doi:10.6342/NTU201901036

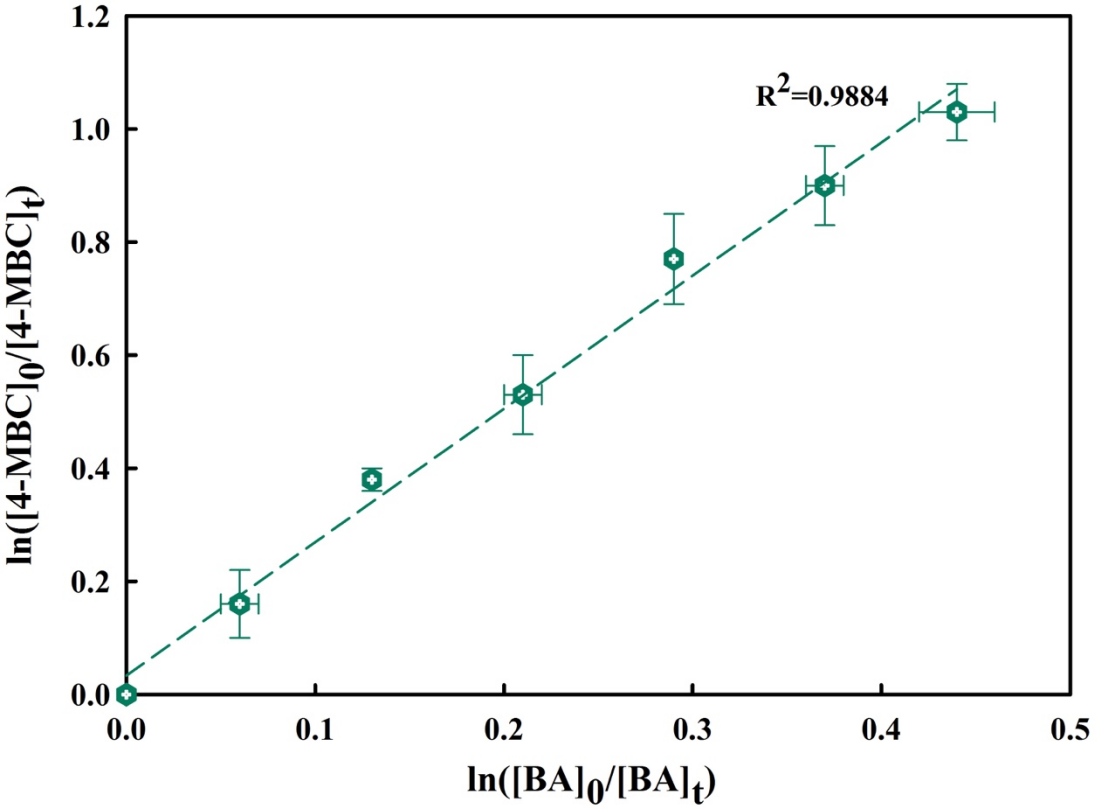

Figure 9. Determination of the reaction rate constant of $SO_4^{-\bullet}$ with 4-MBC. Experimental conditions: $[4\text{-MBC}]_0$ = [benzoic acid] = 3.9 μM, $[\text{persulfate}]_0$ = 420 μM, [TBA] = 42 mM, initial pH = 7.0.

doi:10.6342/NTU201901036

4.5 Final product of persulfate

In the UV/persulfate process, SO_4^{-}• is generated during the UV activation of persulfate. Subsequently, sulfate anions will be generated by electron transfer from 4-MBC to SO_4^{-}•. The conversion ratio of persulfate to sulfate anions can be calculated according to the following equation (Eq. 23) [44].

$$Conversion\ ratio(\%) = \frac{[sulfate\ anion]}{2[persulfate]} \times 100\% \qquad \text{Eq. 23}$$

The relationship between 4-MBC degradation and sulfate anion formation (as indicated by the conversion ratio) over time is shown in Figure 10. As expected, while 4-MBC was degraded, the persulfate conversion ratio continuously increased with reaction time for 10 min. After 10 min of irradiation, the persulfate conversion ratio increased to approximately 100% at persulfate concentrations of 2.1 mM and 42 μM. Thus, the results demonstrated that all the persulfate used in this study was almost completely transformed into sulfate anions after the reaction. A similar trend has also been noted in previous studies [40, 44]. However, the complete transformation of persulfate in the first 10 min also suggested that the reaction between the radical species (SO_4^{-}•) and 4-MBC mainly occurred within this time period. Therefore, the remaining 4-MBC was not further degraded, and equilibrium was reached after 10 min.

doi:10.6342/NTU201901036

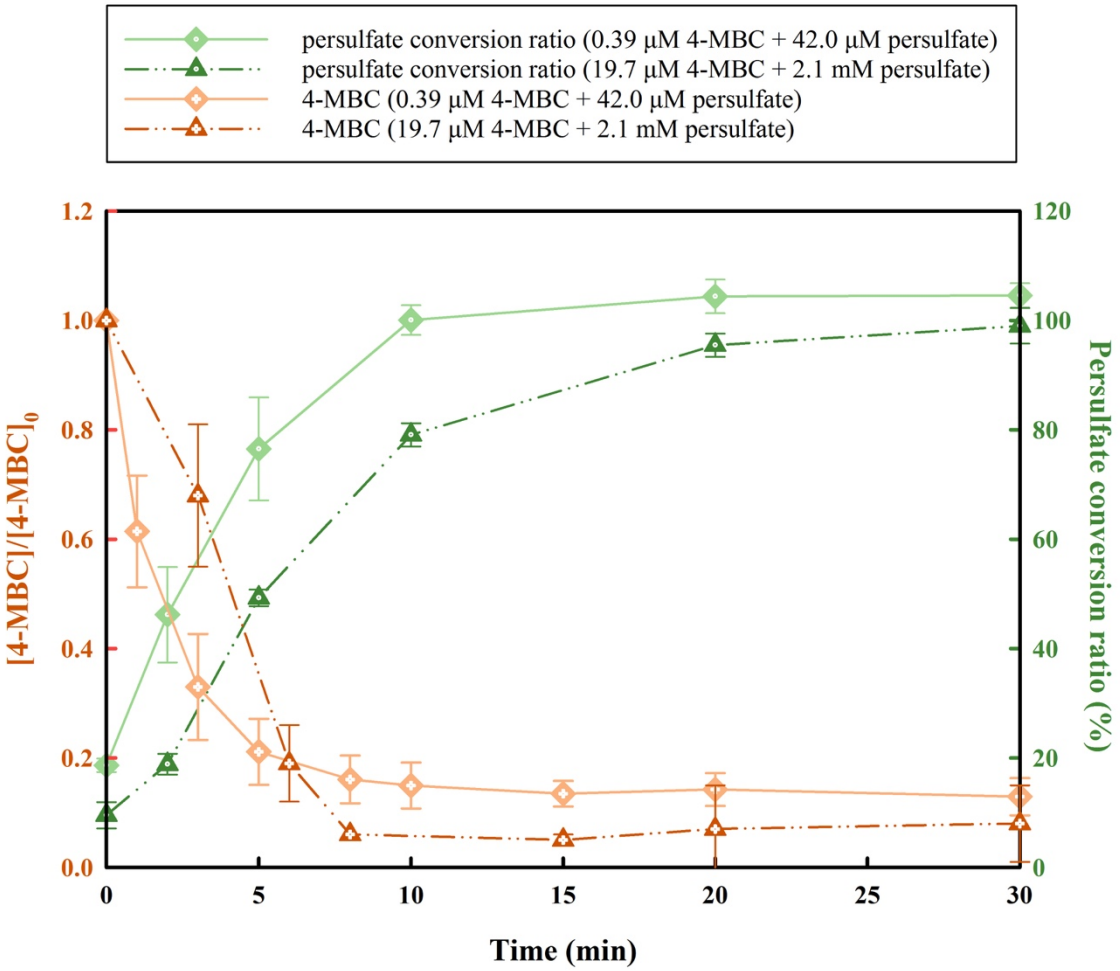

Figure 10. Persulfate conversion ratio during UV/persulfate degradation of 4-MBC. Experimental conditions: (1) $[4\text{-MBC}]_0$ = 0.39 μM and $[\text{persulfate}]_0$ = 42 μM; (2) $[4\text{-MBC}]_0$ = 19.7 μM and $[\text{persulfate}]_0$ =2.1 mM; initial pH= 7.

doi:10.6342/NTU201901036

4.6 Transformation products of 4-MBC

To explore the transformation products during 4-MBC degradation in the UV/persulfate process, an experiment was carried out at a high 4-MBC concentration (19.7 μM) to facilitate the detection of transformation products. The molar concentration ratio of persulfate to 4-MBC remained the same as that in the degradation kinetics study in the previous section 4.5. In addition to the higher concentrations of 4-MBC and persulfate, the reaction time was extended to 60 min. According to the product analysis, two proposed pathways were found in 4-MBC degradation. One pathway is hydroxylation, and the other is demethylation. The hypothetical pathways and time-dependent formation of 4-MBC transformation products are illustrated in Figure 11 and Figure 12, respectively. The detailed chromatographic and mass spectral information for the transformation products are listed in Table S1, Figure S3 and Figure S4. The detection of P1 with an m/z of 271 demonstrated that hydroxylation occurred during 4-MBC degradation in the UV/persulfate process. Hydroxylation frequently occurrs during activation of the persulfate reaction, based on previous published work [45, 46, 50, 56, 58-60]. Moreover, the detection of P2 with an m/z of 242 indicated that demethylation also occurred during 4-MBC degradation in the UV/persulfate process. A previous study has also reported that the possible degradation mechanism of bisphenol A during a SO_4^{-}•-based oxidation process involves demethylation [61].

doi:10.6342/NTU201901036

In the previous section (4.5), we concluded that the radical reaction between $SO_4^{-\bullet}$ and 4-MBC happened only in the first 10 min. However, in Figure 12, we found that the intensities of the byproducts P1 and P2 continuously decreased after 10 min of reaction time. This result implied that P1 and P2 were photolyzed by UV irradiation and that their degradation after 10 min is mainly attributed to direct UV photolysis.

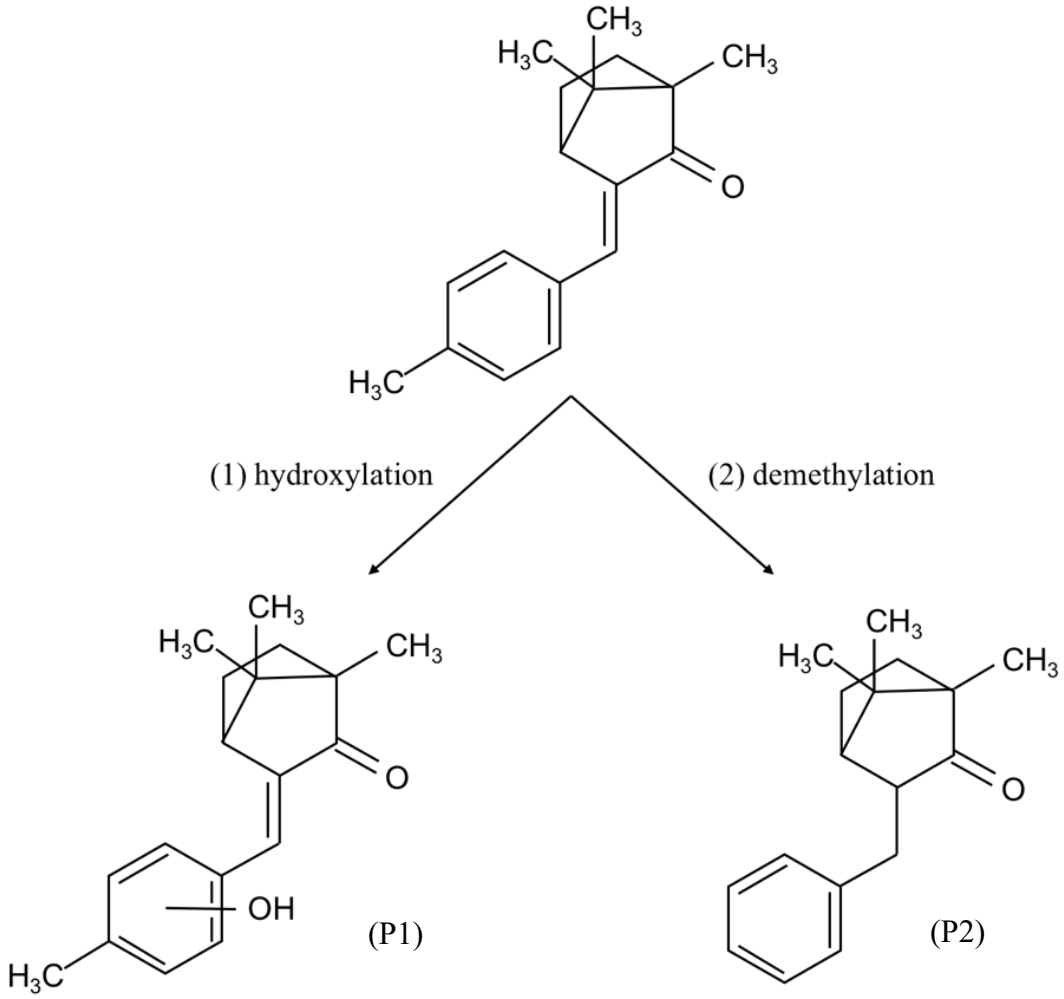

Figure 11. Hypothetical pathways of 4-MBC byproduct formation in the UV/persulfate process.

doi:10.6342/NTU201901036

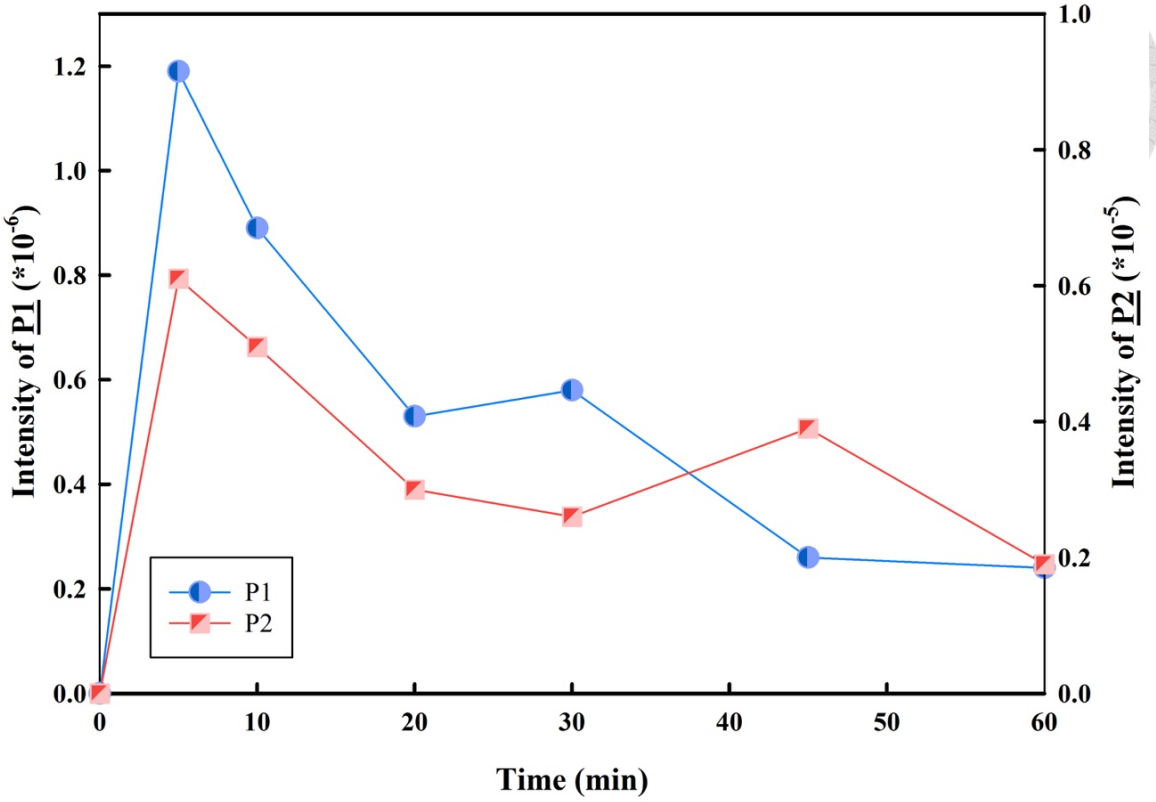

Figure 12. Formation of transformation products in the UV/persulfate process.

doi:10.6342/NTU201901036

4.7 Toxicity

To observe the change in toxicity of 4-MBC during the UV/persulfate process, the initial 4-MBC and persulfate concentrations were raised to fifty times those used in the degradation kinetics experiments (the same elevated conditions as in section 4.6). Moreover, to distinguish the source of toxicity, the experiments were carried out under three conditions, including UV irradiation alone, persulfate dark oxidation and the UV/persulfate process. The changes in toxicity via 4-MBC degradation are shown in Figure 13 and Figure 14. The results from the control experiments (Figure 13) show that the toxicity remained unchanged under both UV irradiation alone and persulfate dark oxidation. However, increased toxicity was observed in the UV/persulfate process (Figure 14): the toxicity continuously increased during the first 20 min, remained at the same level for ten minutes, and then decreased after 30 min of reaction time. A similar trend was reported in a previous work, which indicated that the degradation of sulfamethoxazole exhibited acute toxicity to *Vibrio fischeri* [60]. Both trimethoprim and sulfamethoxazole also showed a higher inhibitory effect on the luminescent bacterium *Vibrio qinghaiensis* after the UV/persulfate process [62]..

The rising toxicity during the UV/persulfate process may be derived from the formation of transformation products that are more toxic than 4-MBC itself. To explore the source of toxicity during 4-MBC degradation, we tentatively compared the toxicity

doi:10.6342/NTU201901036

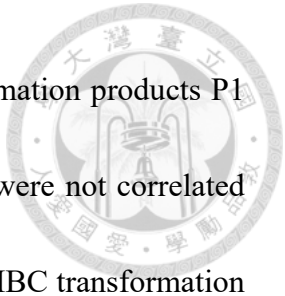

results (Figure 14) with the formation trend of the detected transformation products P1 and P2 (Figure 12). However, the P1 and P2 formation tendencies were not correlated with the toxicity trend. Hence, it is supposed that other unknown 4-MBC transformation products gave rise to the increase in toxicity. However, as stated in the previous section (4.5), the complete transformation between persulfate and sulfate anion in the first 10 min suggested that after 10 min of reaction time, direct UV photolysis would become the dominant mechanism in the system. However, our toxicity results (Figure 14) show that the toxicity continued to change after 10 min of reaction time; which implied that the unknown 4-MBC transformation products were possibly more photolabile to UV irradiation than 4-MBC itself and that the photodegradation of these unknown products resulted in the toxicity change after 10 min. In addition, the formation of transformation products and the change in toxicity indicated that 4-MBC was not completely mineralized at the end of the reaction.

doi:10.6342/NTU201901036

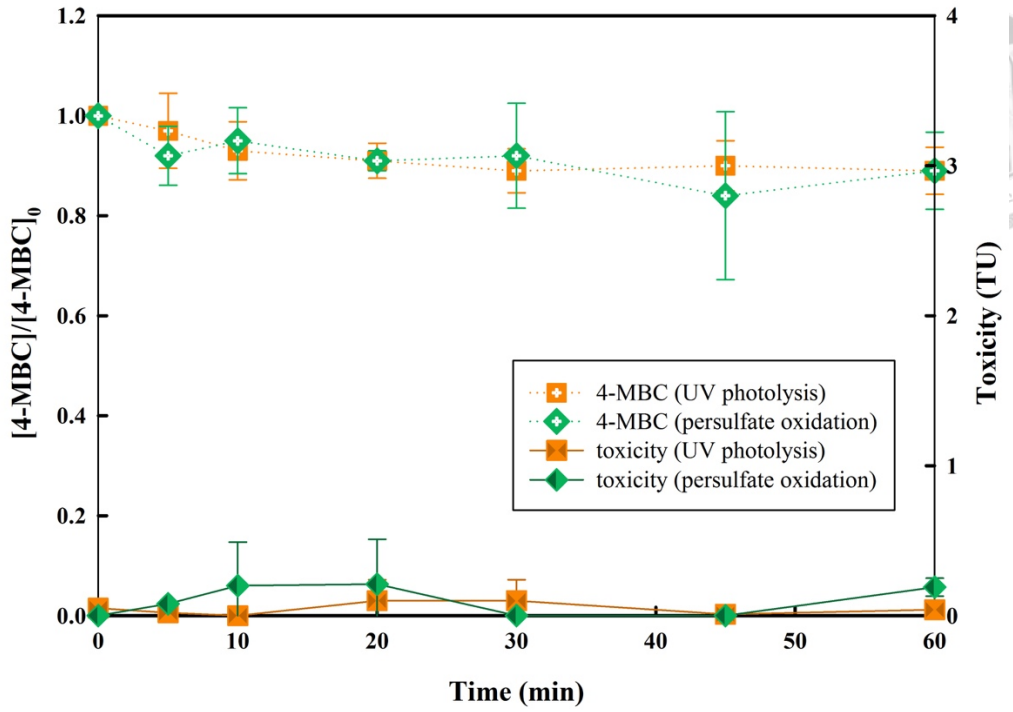

Figure 13. Change in toxicity during 4-MBC degradation under UV irradiation alone and persulfate dark oxidation. Experimental conditions: $[4\text{-MBC}]_0$ = 19.7 μM, $[\text{persulfate}]_0$ = 2.1 mM, initial pH = 7.

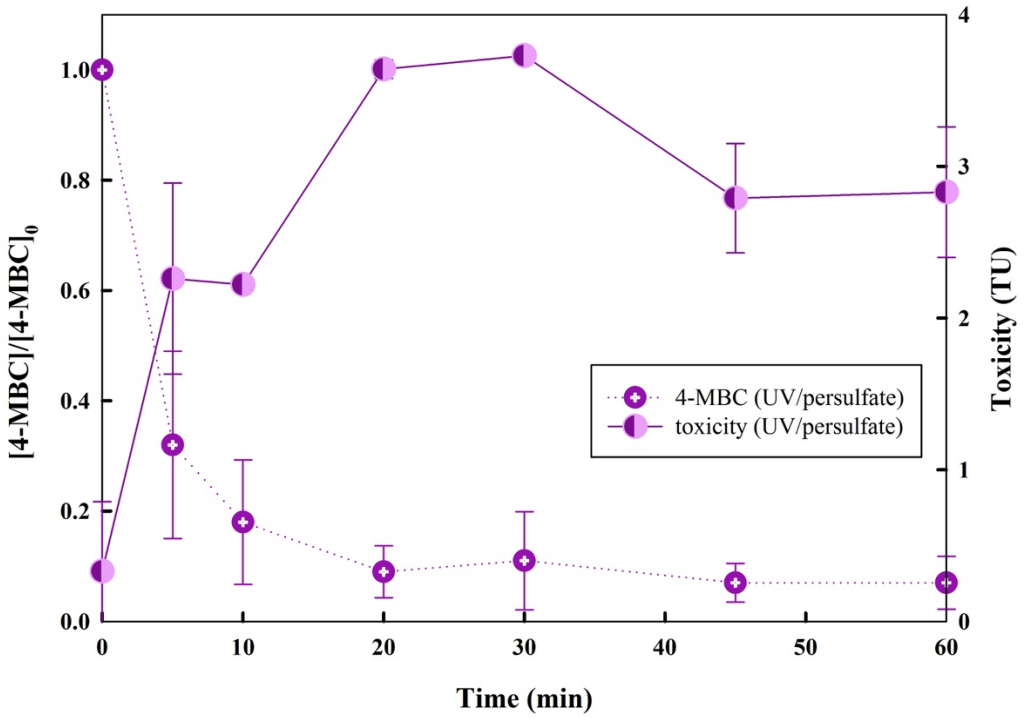

Figure 14. Change in toxicity and 4-MBC degradation with reaction time in the UV/persulfate process. Experimental conditions: $[4\text{-MBC}]_0$ = 19.7 μM, $[\text{persulfate}]_0$ = 2.1 mM, initial pH = 7.

doi:10.6342/NTU201901036

4.8 Effect of swimming pool water

To assess the performance of the UV/persulfate process on 4-MBC degradation in a practical application, outdoor swimming pool water was set as the background matrix. The characteristics of the outdoor swimming pool water are summarized in Table 7. Figure 15 shows the degradation of 4-MBC in outdoor swimming pool water and DI water under UV/persulfate conditions. 4-MBC degradation was significantly attenuated in the outdoor swimming pool water.

To differentiate the factors resulting in the declining degradation efficiency, the experiments were divided to consider two dimensions: one factor was the effect of inorganic anions, and the other was the effect of dissolved organic matter (DOM). Based on our sampling data (Table 7), Cl^- and SO_4^{2-} are the two most abundant anion constituents in outdoor swimming pool water. Hence, these two compounds were added to DI water to mimic the high inorganic anion concentration of outdoor swimming pools, while DOM was solely added to DI water in other samples. The amounts of Cl^-, SO_4^{2-} and DOM adding to the DI water were selected to simulate real swimming pool water (Table 8). Figure 16 shows that the 4-MBC removal was nearly the same in the real and ion-amended synthetic swimming pool water. However, adding DOM to DI water had an insignificant influence on the 4-MBC removal efficiency. These results indeed narrowed down the possible factors that led to the lower degradation efficiency of 4-MBC. Thus, it

doi:10.6342/NTU201901036

can be hypothesized that the inorganic anions, Cl^- and SO_4^{2-} are the major inhibiting factors. Figure S5 demonstrates the 4-MBC removal in the present of different inorganic anions added separately to DI water.

To further discriminate between Cl^- and SO_4^{2-} to identify the main inhibitory effect on degradation efficiency, experiments with various concentrations of Cl^- and SO_4^{2-} in DI water were performed. The experimental conditions are shown in Table 9. Figure 17 plots the graph of the removal of 4-MBC in the presence of different concentrations of anions. The presence of SO_4^{2-} slightly affected the degradation of 4-MBC at all concentrations; however, the existence of Cl^- exhibited a remarkable inhibitory impact, especially at higher Cl^- concentrations. For further confirmation, UV/persulfate experiments in outdoor swimming pool water spiked with additional Cl^- and SO_4^{2-} were also carried out and could be divided into three categories, as shown in Table 10: Cl^- addition only, SO_4^{2-} addition only and both Cl^- and SO_4^{2-} addition. Figure 18 shows the 4-MBC removal under these three conditions. The results corresponded with the experiments conducted in DI water: the influence of Cl^- on 4-MBC degradation in the UV/ persulfate process was more significant than that of SO_4^{2-}. The severe inhibitory effect of Cl^- has also been reported in the previous studies [46, 54, 56].

Cl^- reacts with $SO_4^{-\bullet}$ and yields reactive species such as $Cl\bullet$, $Cl_2^{-\bullet}$, and $ClHO^{-\bullet}$ through complicated chain reactions (Eq. 24-26). The formation of these radials could

doi:10.6342/NTU201901036

suppress the reaction due to their lower redox potentials than that of SO_4^{-}• [63-65]. Furthermore, as mentioned in section 4.5, SO_4^{2-} is expected to be the final product of persulfate oxidation and does not react directly with SO_4^{-}•. Therefore, the presence of SO_4^{2-} resulted in less inhibition of 4-MBC degradation in the UV/persulfate process.

$$Cl^- + SO_4^- \bullet \rightarrow Cl \bullet + SO_4^{2-} \qquad k = 3.0 \times 10^8\ M^{-1}s^{-1} \qquad \text{Eq. 24}$$

$$Cl \bullet + Cl^- \rightarrow Cl_2^- \bullet \qquad k = 8.0 \times 10^9\ M^{-1}s^{-1} \qquad \text{Eq. 25}$$

$$Cl_2^- \bullet + OH^- \rightarrow ClOH^- \bullet + Cl^- \qquad k = 2.0 \times 10^7\ M^{-1}s^{-1} \qquad \text{Eq. 26}$$

doi:10.6342/NTU201901036

Table 7. The characteristics of outdoor swimming pool water.

	Cl^-	NO_3^-	PO_4^{3-}	SO_4^{2-}	DOM
Concentration (ppm)	20.8	2.3	n.a	9.8	0.4

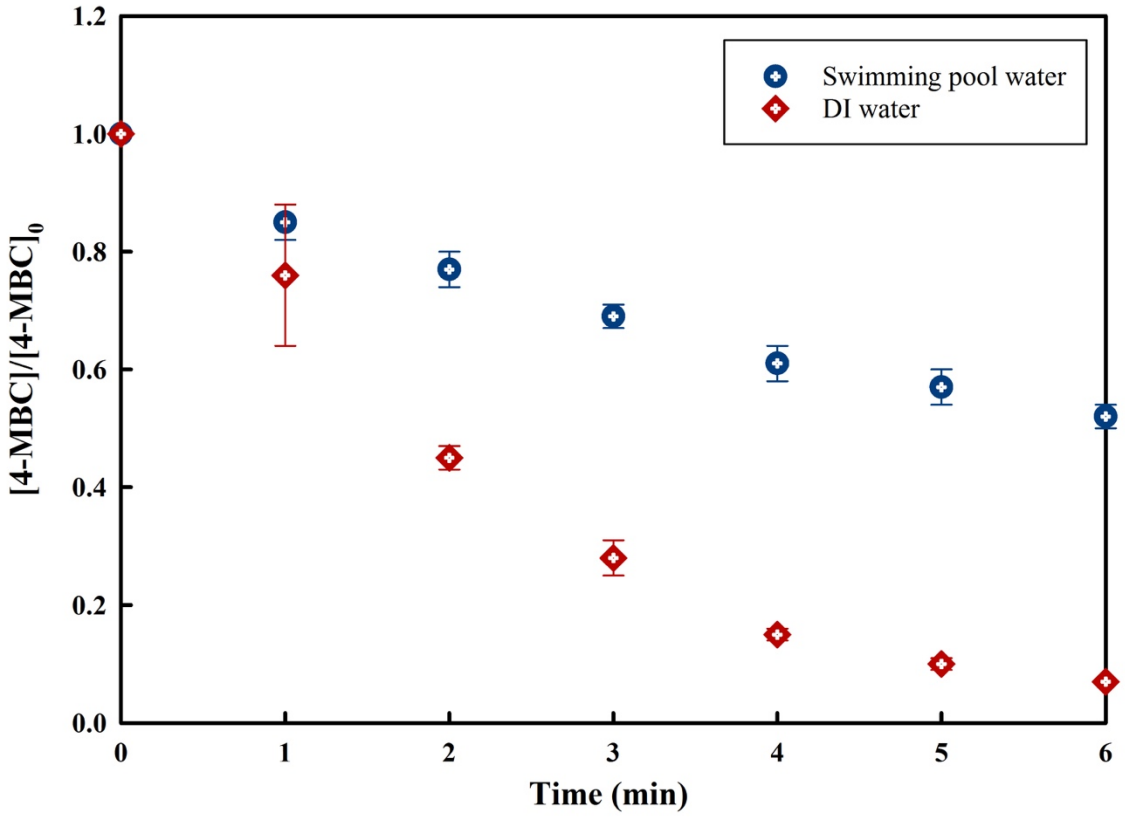

Figure 15. Effect of different water matrices on 4-MBC degradation. Experimental conditions: $[4\text{-MBC}]_0$ = 0.39 μM, $[\text{persulfate}]_0$ = 42 μM, initial pH = 7.0, reaction time = 6 min.

doi:10.6342/NTU201901036

Table 8. The chloride and sulfate ion concentrations in different water matrices.

	Cl^- (ppm)	SO_4^{2-} (ppm)	DOM (ppm)
DI water	-	-	-
Swimming pool water	20.8	9.8	0.4
Synthetic swimming pool water (ion) (DI + Cl^- + SO_4^{2-})	20	10	-
Synthetic swimming pool water (DOM) (DI + DOM)	-	-	0.4

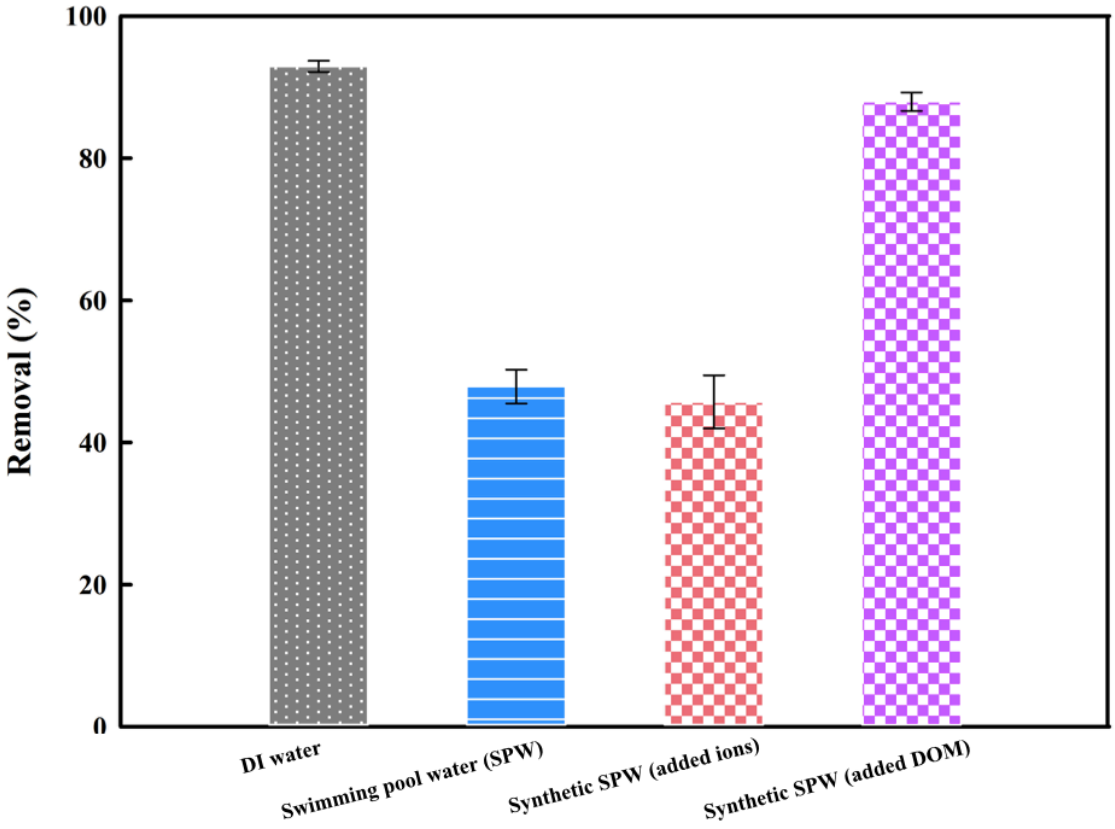

Figure 16. Removal of 4-MBC in different water matrices. Experimental conditions: $[4\text{-MBC}]_0$ = 0.39 μM, $[\text{persulfate}]_0$ = 42 μM, initial pH = 7.0, reaction time = 6 min.

doi:10.6342/NTU201901036

Table 9. The different chloride and sulfate ion concentrations added to DI water.

	Cl^- (ppm)			SO_4^{2-} (ppm)		
DI water	-			-		
DI + Cl^-	10	20	50	-		
DI + SO_4^{2-}	-			5	10	20

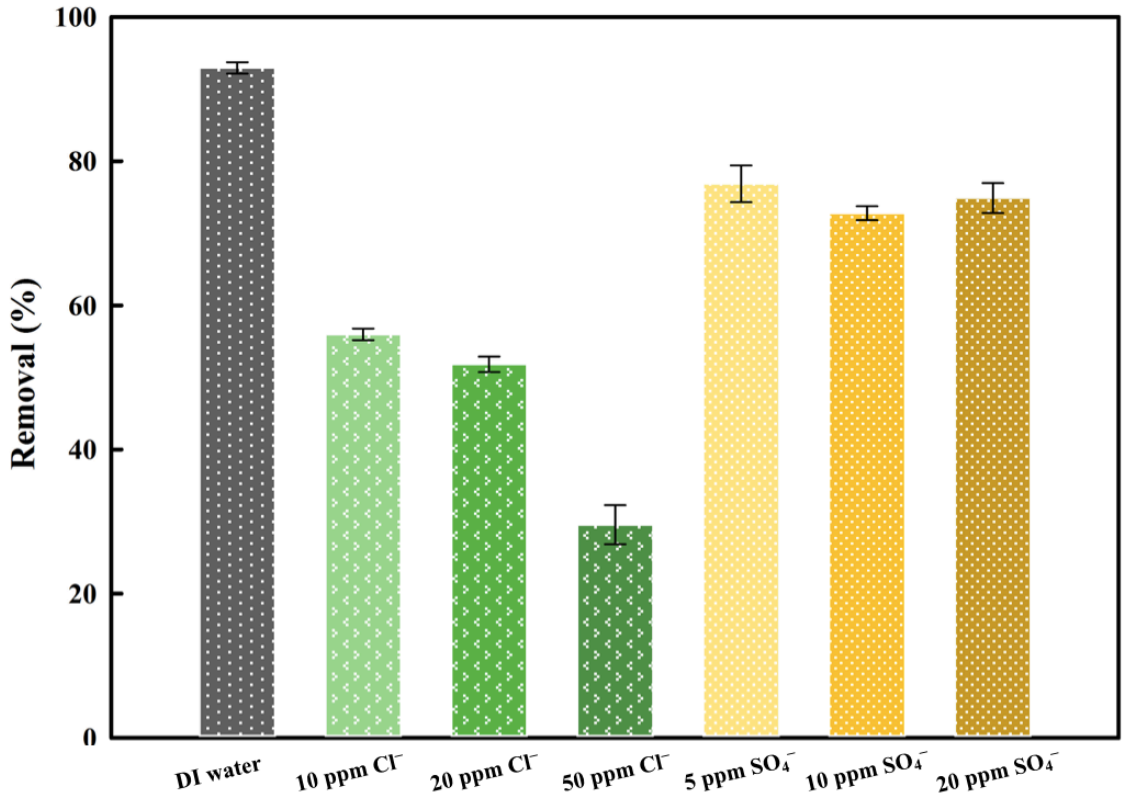

Figure 17. Removal of 4-MBC in DI water with different concentration of inorganic anions. Experimental conditions: $[4\text{-MBC}]_0$ = 0.39 μM, $[\text{persulfate}]_0$ = 42 μM, initial pH = 7.0, reaction time = 6 min.

doi:10.6342/NTU201901036

Table 10. The different chloride and sulfate ion concentrations added to outdoor swimming pool water.

	Cl^- (ppm)	SO_4^{2-} (ppm)
Swimming pool water	20.8	9.8
Swimming pool water + Cl^- + SO_4^{2-}	40.8	19.8
Swimming pool water + Cl^-	40.8	9.8
Swimming pool water + SO_4^{2-}	20.8	19.8

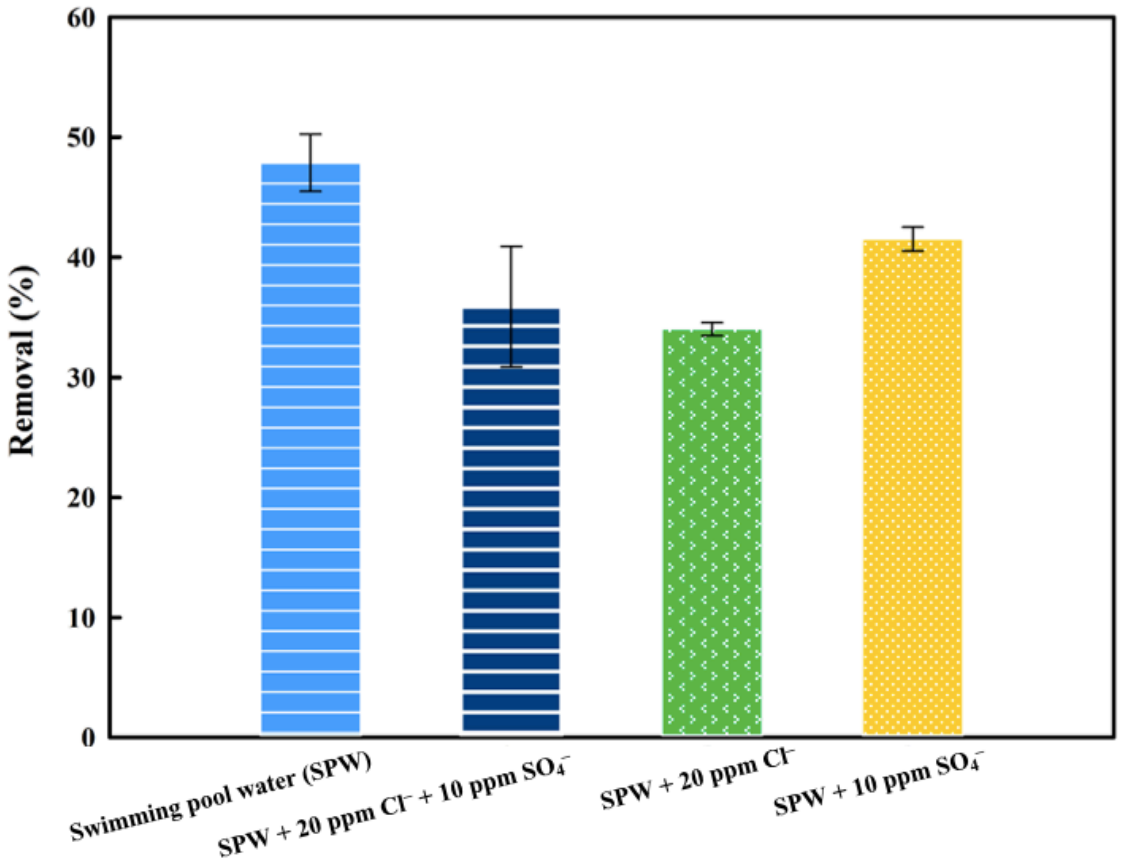

Figure 18. Removal of 4-MBC in swimming pool water with different concentrations of inorganic anions. Experimental conditions: $[4\text{-MBC}]_0$ = 0.39 μM, $[\text{persulfate}]_0$ = 42 μM, initial pH = 7.0, reaction time = 6 min.

doi:10.6342/NTU201901036

Chapter 5 Conclusions and Environmental Implication

The conclusions drawn from this work include the following:

I. The UV/persulfate process significantly enhances the degradation of 4-MBC.

- Upon UV photolysis alone, 4-MBC experienced only photoisomerization between (E)- and (Z)-4-MBC.
- Under the conditions of $[4\text{-MBC}]_0$ = 0.39 μM, $[\text{persulfate}]_0$ = 42 μM and initial pH = 7, 4-MBC was nearly completely decomposed within 6 min.

II. The persulfate dosage and solution pH affect the 4-MBC degradation rate in the UV/persulfate process.

- As the persulfate dosage ranged from 4.2 μM to 42 μM, k_{obs} increased from 4.0×10^{-2} to 44.8×10^{-2} min^{-1}.
- k_{obs} remained approximately constant in acidic (pH 5) and neutral solutions, but significantly decreased in basic conditions (pH 9).

III. SO_4^{-}• is the dominant radical responsible for 4-MBC degradation in the UV/persulfate process.

- The second-order rate constant of SO_4^{-}• with 4-MBC was calculated to be $(2.95 \pm 0.05) \times 10^9$ M^{-1} s^{-1}.

IV. Transformation products of 4-MBC are generated during the UV/persulfate process.

doi:10.6342/NTU201901036

- The proposed transformation pathways of 4-MBC involved hydroxylation and demethylation.
- The formation of unknown transformation products resulted in the rising toxicity and indicated that 4-MBC was not completely mineralized at the end of the reaction.

V. The removal of 4-MBC decreased from 93% to 48% in swimming pool water.

- Inorganic anions are the major inhibiting factors especially Cl^-.

Recommendations for future work:

I. The transformation products found in the present work were not correlated with the toxicity trend. Further investigation of the unknown transformation products resulting in the rising toxicity should be carried out.

II. The removal of 4-MBC in the UV/persulfate process should be conducted in a more complicated water matrix (e.g., wastewater) to understand the effects of other constituents.

Environmental implication:

Although inorganic anions attenuate the 4-MBC degradation in the UV/persulfate process, removing inorganic anions would be an important pretreatment step if this UV/persulfate process were to be used in the real wastewater environments. However, investigations on the effect of the coexisting substances, as well as further

doi:10.6342/NTU201901036

ecotoxicological tests, should be conducted carefully and comprehensively before this technology is utilized in practical applications.

doi:10.6342/NTU201901036

Chapter 6 Reference

1. EPA, U.S., White Paper Aquatic Life Criteria For Contaminants Of Emerging Concern. 2008.
2. Alistair B.A. Boxall, Murray A. Rudd, Bryan W. Brooks, Daniel J. Caldwell, Kyungho Choi, Silke Hickmann, Elizabeth Innes, Kim Ostapyk, Jane P. Staveley, Tim Verslycke, Gerald T. Ankley, Karen F. Beazley, Scott E. Belanger, Jason P. Berninger, Pedro Carriquiriborde, Anja Coors, Paul C. DeLeo, Scott D. Dyer, Jon F. Ericson, François Gagné, John P. Giesy, Todd Gouin, Lars Hallstrom, Maja V. Karlsson, D. G. Joakim Larsson, James M. Lazorchak, Frank Mastrocco, Alison McLaughlin, Mark E. McMaster, Roger D. Meyerhoff, Roberta Moore, Joanne L. Parrott, Jason R. Snape, Richard Murray-Smith, Mark R. Servos, Paul K. Sibley, Jürg Oliver Straub, Nora D. Szabo, Edward Topp, Gerald R. Tetreault, Vance L. Trudeau, and Glen Van Der Kraak, Pharmaceuticals and personal care products in the environment: what are the big questions? Environ Health Perspect, 2012. 120(9): p. 1221−1229.
3. Marianne E. Balmer, Hans-Rudolf Buser, Markus D. Müller, and Thomas Poiger, Ocurrence of Some Organic UV Filters in Wastewater, in Surface Waters, and in Fish from Swiss Lakes. Environmental Science & Technology, 2005. 39: p. 953−962.
4. Hans-Rudolf Buser, Markus D. Müller, Marianne E. Balmer, Thomas Poiger, and Ignaz J. Buerge, Stereoisomer Composition of the Chiral UV Filter 4-Methylbenzylidene Camphor in Environmental Samples. Environmental Science & Technology, 2005. 39: p. 3013−3019.
5. Dimosthenis L. Giokas, Vasilios A. Sakkas and Triantafyllos A. Albanis, Determination of residues of UV filters in natural waters by solid-phase extraction

doi:10.6342/NTU201901036

coupled to liquid chromatography–photodiode array detection and gas chromatography–mass spectrometry. Journal of Chromatography A, 2004. 1026: p. 289−293.

6. Cuderman, P. and E. Heath, Determination of UV filters and antimicrobial agents in environmental water samples. Analytical and Bioanalytical Chemistry, 2007. 387: p. 1343−1350.
7. M. Silvia Díaz-Cruz, Pablo Gago-Ferrero, Marta Llorca and Damià Barceló, Analysis of UV filters in tap water and other clean waters in Spain. Analytical and Bioanalytical Chemistry, 2012. 402: p. 2325−2333.
8. Anna Jurado, Pablo Gago-Ferrero, Enric Vàzquez-Sun̆é, Jesus Carrera, Estanislao Pujades, M.Silvia Díaz-Cruz and Damià Barceló, Urban groundwater contamination by residues of UV filters. Journal of Hazardous Materials, 2014. 271: p. 141−149.
9. Philipp Emnet, Sally Gaw, Grant Northcott, Bryan Storey and Lisa Graham, Personal care products and steroid hormones in the Antarctic coastal environment associated with two Antarctic research stations, McMurdo Station and Scott Base. Environmental Research, 2015. 136: p. 331−342.
10. Thomas Poiger, Hans-Rudolf Buser, Marianne E. Balmer, Per-Anders Bergqvist and Markus D. Müller, Occurrence of UV filter compounds from sunscreens in surface waters: regional mass balance in two Swiss lakes. Chemosphere, 2004. 55: p. 951−963.
11. Mayumi Allinson, Yutaka Kameda, Kumiko Kimura and Graeme Allinson, Occurrence and assessment of the risk of ultraviolet filters and light stabilizers in Victorian estuaries. Environmental Science and Pollution Research, 2018. 25: p. 12022−12033.
12. Mirabelle M.P. Tsui, H.W. Leung, Tak-Cheung Wai, Nobuyoshi Yamashita, Sachi

doi:10.6342/NTU201901036

Taniyasu, Wenhua Liu, Paul K.S. Lam and Margaret B. Murphy, Occurrence, distribution and ecological risk assessment of multiple classes of UV filters in surface waters from different countries. Water Research, 2014. 67: p. 55−65.

13. K. H. Langford and K. V. Thomas, Inputs of chemicals from recreational activities into the Norwegian coastal zone. Journal of Environmental Monitoring, 2008. 10: p. 894−898.
14. A. Sánchez Rodríguez, M. Rodrigo Sanz and J.R. Betancort Rodríguez, Occurrence of eight UV filters in beaches of Gran Canaria (Canary Islands). An approach to environmental risk assessment. Chemosphere, 2015. 131: p. 85−90.
15. Petra Y. Kunz and Karl Fent, Multiple hormonal activities of UV filters and comparison of *in vivo* and *in vitro* estrogenic activity of ethyl-4-aminobenzoate in fish. Aquatic Toxicology, 2006. 79: p. 305−324.
16. William H. Glaze , Joon-Wun Kang and Douglas H. Chapin, The chemistry of water treatment processes involving ozone, hydrogen peroxide and ultraviolet radiation. Ozone Science & Engineering, 1987. 9: p. 335−352.
17. David B. Miklos, Christian Remy, Martin Jekel, Karl G. Linden, Jörg E. Drewes and Uwe Hübner, Evaluation of advanced oxidation processes for water and wastewater treatment – A critical review. Water Research, 2018. 139: p. 118−131.
18. Brian P. Chaplin, Critical review of electrochemical advanced oxidation processes for water treatment applications. Environmental Science Process & Impacts, 2014. 16: p. 1182−1203.
19. Yang Deng and Renzun Zhao, Advanced Oxidation Processes (AOPs) in Wastewater Treatment. Current Pollution Reports, 2015. 1: p. 167−176.
20. Tugba Olmez-Hanci and Idil Arslan-Alaton, Comparison of sulfate and hydroxyl radical based advanced oxidation of phenol. Chemical Engineering Journal, 2013.

doi:10.6342/NTU201901036

224: p. 10−16.

21. George V. Buxton, Clive L. Greenstock, W. Phillip Helman and Alberta B. Ross, Critical Review of rate constants for reactions of hydrated electrons, hydrogen atoms and hydroxyl radicals (·OH/·O^-) in Aqueous Solution. Journal of Physical and Chemical Reference Data, 1988. 17: p. 513−886.
22. P. Neta, Robert E. Huie, and Alberta B. Ross, Rate Constants for Reactions of Inorganic Radicals in Aqueous Solution. Journal of Physical and Chemical Reference Data, 1988. 17: p. 1027−1284.
23. V.A. Sakkas, P. Calza, M. Azharul Islam, C. Medana, C. Baiocchi, K. Panagiotou and T. Albanis, TiO_2/H_2O_2 mediated photocatalytic transformation of UV filter 4-methylbenzylidene camphor (4-MBC) in aqueous phase: Statistical optimization and photoproduct analysis. Applied Catalysis B: Environmental, 2009. 90: p. 526−534.
24. L. Hernańdez-Leal, H. Temmink, G. Zeeman and C.J.N. Buisman, Removal of micropollutants from aerobically treated grey water via ozone and activated carbon. Water Research, 2011. 45: p. 2887−2896.
25. Ce´cile Plagellat, Thomas Kupper, Reinhard Furrer, Luiz Felippe de Alencastro, Dominique Grandjean and Joseph Tarradellas, Concentrations and specific loads of UV filters in sewage sludge originating from a monitoring network in Switzerland. Chemosphere, 2006. 62: p. 915−925.
26. N. Negreira, I. Rodríguez and E. Rubí, R. Cela, Optimization of pressurized liquid extraction and purification conditions for gas chromatography-mass spectrometry determination of UV filters in sludge. Journal of Chromatography A, 2011. 1218: p. 211−217.
27. David Sánchez-Quiles and Antonio Tovar-Sánchez, Are sunscreens a new environmental risk associated with coastal tourism? Environment International,

doi:10.6342/NTU201901036

2015. 83: p. 158−170.

28. Hans-Rudolf Buser, Marianne E. Balmer, Peter Schmid and Martin Kohler, Occurrence of UV Filters 4-Methylbenzylidene Camphor and Octocrylene in Fish from Various Swiss Rivers with Inputs from Wastewater Treatment Plants. Environmental Science & Technology, 2006. 40: p. 1427−1431.
29. NR Janjua, B Kongshoj, A-M Andersson and HC Wulf, Sunscreens in human plasma and urine after repeated whole-body topical application. J Eur Acad Dermatol Venereol, 2008. 22: p. 456−461.
30. Margret Schlumpf, Karin Kypke, Claudia C. Vökt, Monika Birchler, Stefan Durrer, Oliver Faass, Colin Ehnes, Michaela Fuetsch, Catherine Gaille, Manuel Henseler, Luke Hofkamp, Kirsten Maerkel, Sasha Reolon, Armin Zenker, Barry Timms, Jesus A. F. Tresguerres and Walter Lichtensteiger, Endocrine Active UV Filters: Developmental Toxicity and Exposure Through Breast Milk. CHIMIA International Journal for Chemistry, 2008. 62: p. 345−351.
31. Margret Schlumpf, Beata Cotton, Marianne Conscience, Vreni Haller, Beate Steinmann, and Walter Lichtensteiger, *In Vitro* and *in Vivo* Estrogenicity of UV Screens. Environmental Health Perspectives, 2001. 109: p. 230−244.
32. Anja Klann, Gregor Levy, Ilka Lutz, Christian Müller, Werner Kloas and Jan-Peter Hildebrandt, Estrogen-like effects of ultraviolet screen 3-(4-methylbenzylidene)-camphor (Eusolex 6300) on cell proliferation and gene induction in mammalian and amphibian cells. Environmental Research, 2005. 97: p. 274−281.
33. Margret Schlumpf, Peter Schmid, Stefan Durrer, Marianne Conscience, Kirsten Maerkel, Manuel Henseler, Melanie Gruetter, Ingrid Herzog, Sasha Reolon, Raffaella Ceccatelli, Oliver Faass, Eva Stutz, Hubertus Jarry, Wolfgang Wuttke and Walter Lichtensteiger, Endocrine activity and developmental toxicity of cosmetic

doi:10.6342/NTU201901036

UV filters – an update. Toxicology, 2004. 205: p. 113−122.

34. Vincent Wai Tsun Li, Mei Po Mirabelle Tsui, Xueping Chen, Michelle Nga Yu Hui, Ling Jin, Raymond H. W. Lam, Richard Man Kit Yu, Margaret B. Murphy, Jinping Cheng, Paul Kwan Sing Lam and Shuk Han Cheng, Effects of 4-methylbenzylidene camphor (4-MBC) on neuronal and muscular development in zebrafish (*Danio rerio*) embryos. Environmental Science and Pollution Research, 2016. 23: p. 8275−8285.
35. Dimosthenis L. Giokas, Vasilios A. Sakkas, Triantafyllos A. Albanis and Dimitra A. Lampropoulou, Determination of UV-filter residues in bathing waters by liquid chromatography UV-diode array and gas chromatography–mass spectrometry after micelle mediated extraction-solvent back extraction. Journal of Chromatography A, 2005. 1077: p. 19−27.
36. Enrique Barón, Pablo Gago-Ferrero, Marina Gorga, Ignacio Rudolph, Gonzalo Mendoza, Andrés Mauricio Zapata, Sílvia Díaz-Cruz, Ricardo Barra, William Ocampo-Duque, Martha Páez, Rosa María Darbra, Ethel Eljarrat and Damià Barceló, Occurrence of hydrophobic organic pollutants (BFRs and UV-filters) in sediments from South America. Chemosphere, 2013. 92: p. 309−316.
37. Weixia Huang, Zhiyong Xie, Wen Yan, Wenying Mi and Weihai Xu, Occurrence and distribution of synthetic musks and organic UV filters from riverine and coastal sediments in the Pearl River estuary of China. Marine Pollution Bulletin, 2016. 111: p. 153−159.
38. Isuha Tarazona, Alberto Chisvert and Amparo Salvador, Development of a gas chromatography-mass spectrometry method for the determination of ultraviolet filters in beach sand samples. Analytical methods, 2014. 6: p. 7772−7780.
39. E.J. Behrman and D.H. Dean, Sodium peroxydisulfate is a stable and cheap substitute for ammonium peroxydisulfate (persulfate) in polyacrylamide gel electrophoresis.

doi:10.6342/NTU201901036

Journal of Chromatography B, 1999. 723: p. 325−326.

40. Hisao Hori, Ari Yamamoto, Etsuko Hayakawa, Sachi Taniyasu, Nobuyoshi Yamashita, and Shuzo Kutsuna, Efficient Decomposition of Environmentally Persistent Perfluorocarboxylic Acids by Use of Persulfate as a Photochemical Oxidant. Environmental Science & Technology, 2005. 39: p. 2383−2388.
41. I. M. Kolthoff and I. K. Miller, The Chemistry of Persulfate. I. The Kinetics and Mechanism of the Decomposition of the Persulfate Ion in Aqueous Medium. Journal of the American Chemical Society, 1951. 73 p. 3055−3059.
42. E. Hayon, A. Treinin, and J. Wilf, Electronic Spectra, Photochemistry, and Autoxidation Mechanism of the Sulfite-Bisulfite-Pyrosulfite Systems. The $S0_2^-$, $S0_3^-$, $S0_4^-$, and SO_5^- Radicals. Journal of the American Chemical Society, 1972. 94: p. 47−57.
43. Kun-Chang Huang, Zhiqiang Zhao, George E. Hoag and Amine Dahmani, Philip A. Block, Degradation of volatile organic compounds with thermally activated persulfate oxidation. Chemosphere, 2005. 61: p. 551−560.
44. Yu-qiong Gao, Nai-yun Gao, Yang Deng, Yi-qiong Yang and Yan Ma, Ultraviolet (UV) light-activated persulfate oxidation of sulfamethazine in water. Chemical Engineering Journal, 2012. 195-196: p. 248−253.
45. Antoine Ghauch, Abbas Baalbaki, Maya Amasha, Rime El Asmar and Omar Tantawi, Contribution of persulfate in UV-254 nm activated systems for complete degradation of chloramphenicol antibiotic in water. Chemical Engineering Journal, 2017. 317: p. 1012−1025.
46. Sarita Dhaka, Rahul Kumar, Moonis Ali Khan, Ki-Jung Paeng, Mayur B. Kurade, Sun-Joon Kim and Byong-Hun Jeon, Aqueous phase degradation of methyl paraben using UV-activated persulfate method. Chemical Engineering Journal, 2017. 321: p.

doi:10.6342/NTU201901036

11−19.

47. Qiongfang Wang, Yisheng Shao, Naiyun Gao, Wenhai Chu, Xiang Shen, Xian Lu, Juxiang Chen and Yanping Zhu, Degradation kinetics and mechanism of 2,4-Di-tert-butylphenol with UV/persulfate. Chemical Engineering Journal, 2016. 304: p. 201−208.
48. Yajie Qian, Xin Guo, Yalei Zhang, Yue Peng, Peizhe Sun, Ching-Hua Huang, Junfeng Niu, Xuefei Zhou, and John C. Crittenden, Perfluorooctanoic Acid Degradation Using UV–Persulfate Process: Modeling of the Degradation and Chlorate Formation. Environmental Science & Technology, 2016. 50: p. 772−781.
49. Noor S. Shah, Xuexiang He, Hasan M. Khan, Javed Ali Khan, Kevin E. O'Shea, Dominic L. Boccelli and Dionysios D. Dionysiou, Efficient removal of endosulfan from aqueous solution by UV-C/peroxides: a comparative study. Journal of Hazardous Materials, 2013. 263: p. 584−592.
50. Tim K. Lau, Wei Chu, and Nigel J. D. Graham, The Aqueous Degradation of Butylated Hydroxyanisole by UV/$S_2O_8^{2-}$: Study of Reaction Mechanisms via Dimerization and Mineralization. Environmental Science & Technology, 2007. 41: p. 613−619.
51. Shaodong Hou, Li Ling, Chii Shang, Yinghong Guan and Jingyun Fang, Degradation kinetics and pathways of haloacetonitriles by the UV/persulfate process. Chemical Engineering Journal, 2017. 320: p. 478−484.
52. Xiao-Ying Yu, Zhen-Chuan Bao, and John R. Barker, Free Radical Reactions Involving Cl•, Cl^-•, and SO_4^-• in the 248 nm Photolysis of Aqueous Solutions Containing $S_2O_8^{2-}$ and Cl^-. The Journal of Physical Chemistry A, 2004. 108: p. 295−308.
53. P. Neta, V. Madhavan, Haya Zemel, and Richard W. Fessenden, Rate Constants and

doi:10.6342/NTU201901036

Mechanism of Reaction of $SO_4^{-\bullet}$ with Aromatic Compounds. Journal of the American Chemical Society, 1977. 99: p. 163–164.

54. Congwei Luo, Jin Jiang, Jun Ma, Suyan Pang, Yongze Liu, Yang Song, Chaoting Guan, Juan Li, Yixin Jin and Daoji Wu, Oxidation of the odorous compound 2,4,6-trichloroanisole by UV activated persulfate: Kinetics, products, and pathways. Water Research, 2016. 96: p. 12−21.
55. Alexandra Ioannidi, Zacharias Frontistis and Dionissios Mantzavinos, Destruction of propyl paraben by persulfate activated with UV-A light emitting diodes. Journal of Environmental Chemical Engineering, 2018. 6: p. 2992−2997.
56. Yiqing Zhang, Jiefeng Zhang, Yongjun Xiao, Victor W.C. Chang and Teik-Thye Lim, Kinetic and mechanistic investigation of azathioprine degradation in water by UV, UV/H_2O_2 and UV/persulfate. Chemical Engineering Journal, 2016. 302: p. 526−534.
57. Yuefei Ji, Yan Yang, Lei Zhou, Lu Wang, Junhe Lu, Corinne Ferronato and Jean-Marc Chovelon, Photodegradation of sulfasalazine and its human metabolites in water by UV and UV/peroxydisulfate processes. Water Research, 2018. 133: p. 299−309.
58. Jinshao Ye, Pulin Zhou, Ya Chen, Huase Ou, Juan Liu, Chongshu Li and Qusheng Li, Degradation of 1H-benzotriazole using ultraviolet activating persulfate: Mechanisms, products and toxicological analysis. Chemical Engineering Journal, 2018. 334: p. 1493−1501.
59. Ruochun Zhang, Peizhe Sun, Treavor H. Boyer, Lin Zhao and Ching-Hua Huang, Degradation of Pharmaceuticals and Metabolite in Synthetic Human Urine by UV, UV/H_2O_2, and UV/PDS. Environmental Science & Technology, 2015. 49: p. 3056−3066.
60. Yi Yang, Xinglin Lu, Jin Jiang, Jun Ma, Guanqi Liu, Ying Cao, Weili Liu, Juan Li, Suyan Pang, Xiujuan Kong and Congwei Luo, Degradation of sulfamethoxazole by

doi:10.6342/NTU201901036

UV, UV/H_2O_2 and UV/persulfate (PDS): Formation of oxidation products and effect of bicarbonate. Water Research, 2017. 118: p. 196−207.

61. Jyoti Sharma, I.M. Mishra, Dionysios D. Dionysiou and Vineet Kumar, Oxidative removal of Bisphenol A by UV-C/peroxymonosulfate (PMS): Kinetics, influence of co-existing chemicals and degradation pathway. Chemical Engineering Journal, 2015. 276: p. 193−204.
62. Ruochun Zhang, Yongkui Yang, Ching-Hua Huang, Na Li, Hang Liu, Lin Zhao and Peizhe Sun, UV/H_2O_2 and UV/PDS Treatment of Trimethoprim and Sulfamethoxazole in Synthetic Human Urine: Transformation Products and Toxicity. Environmental Science & Technology, 2016. 50: p. 2573−2583.
63. G. G. Jayson and B. J. Parsons, Some Simple, Highly Reactive, Inorganic Chlorine Derivatives in Aqueous Solution. Journal of the Chemical Society, Faraday Transactions 1: Physical Chemistry in Condensed Phases, 1973. 69: p. 1597−1607.
64. Tomi Nath Das, Reactivity and Role of $SO_5^{\bullet -}$ Radical in Aqueous Medium Chain Oxidation of Sulfite to Sulfate and Atmospheric Sulfuric Acid Generation. The Journal of Physical Chemistry A, 2001. 105: p. 9142−9155.
65. Yi Yang, Joseph J. Pignatello, Jun Ma, and William A. Mitch, Comparison of Halide Impacts on the Efficiency of Contaminant Degradation by Sulfate and Hydroxyl Radical-Based Advanced Oxidation Processes (AOPs). Environmental Science & Technology, 2014. 48: p. 2344−2351.

doi:10.6342/NTU201901036

Supporting information

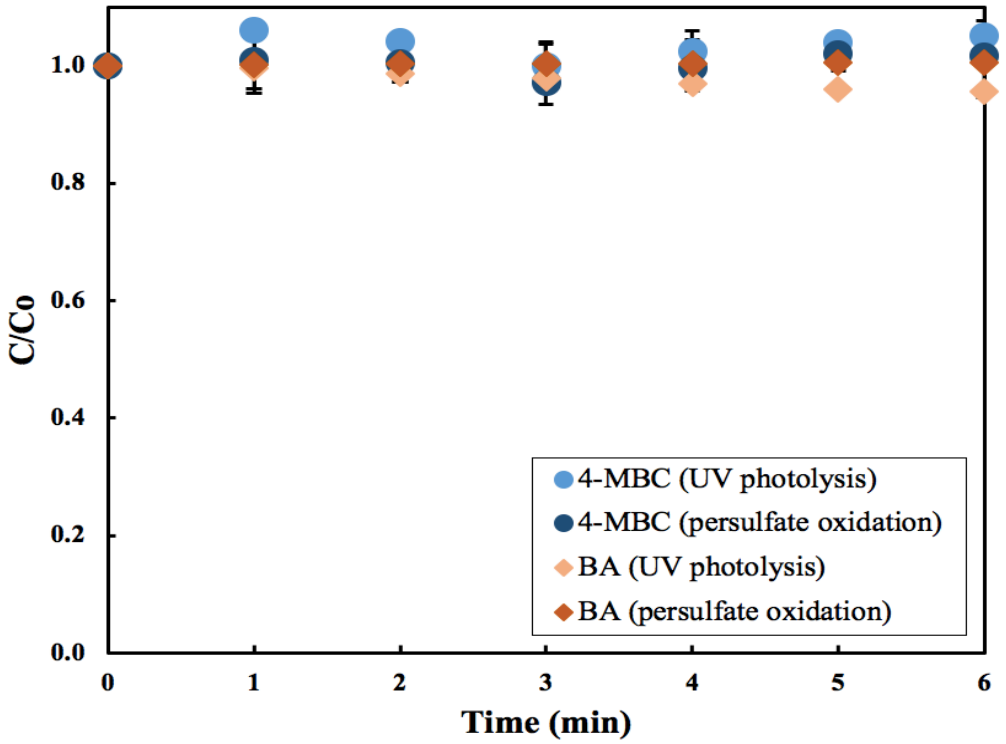

Figure S1. Degradation of 4-MBC and benzoic acid under UV irradiation alone and persulfate dark oxidation.

Table S1. List of transformation products of 4-MBC in the UV/persulfate process as detected by LC-QTOF-MS/MS.

Transformation byproducts	Retention time (min)	Formula	Error (ppm)	Measured m/z $[M+H]^+$
P1	3.75	$C_{18}H_{22}O_2$	-0.8	271.1587
P2	3.97	$C_{17}H_{22}O$	0.7	242.2030

doi:10.6342/NTU201901036

(a)

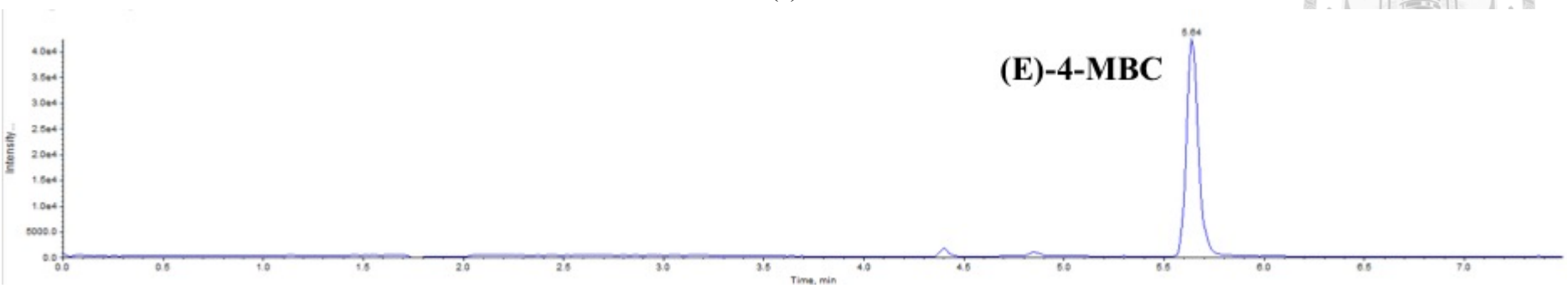

(b)

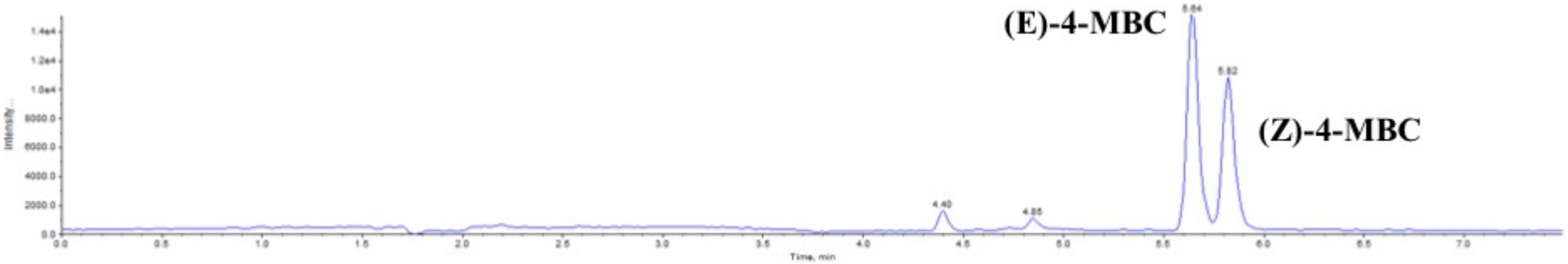

Figure S2. Chromatograms of the (E)- and (Z)-4-MBC: (a) before and (b) after the UV irradiation.

doi:10.6342/NTU201901036

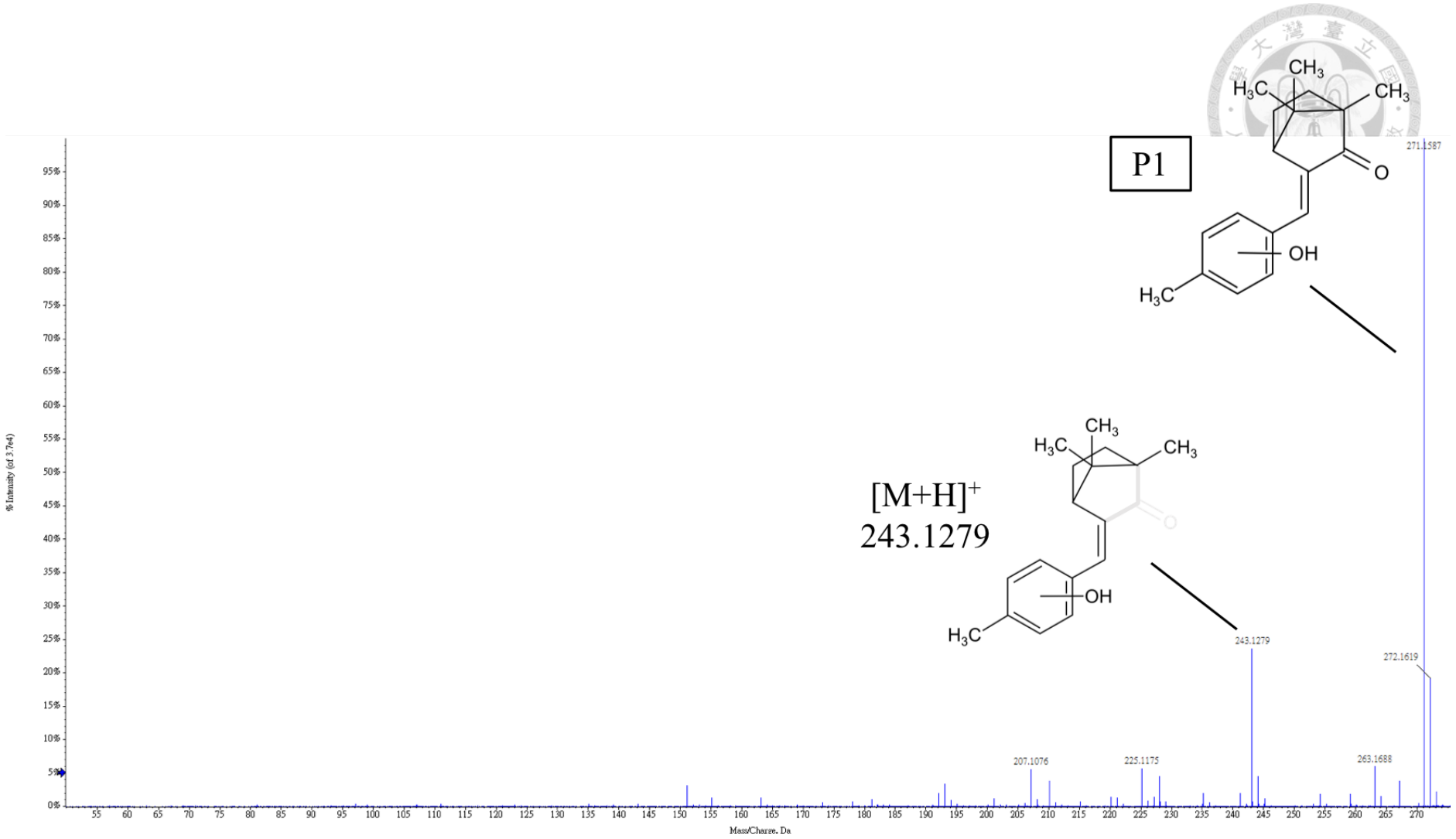

Figure S3. Mass spectrum of P1

doi:10.6342/NTU201901036

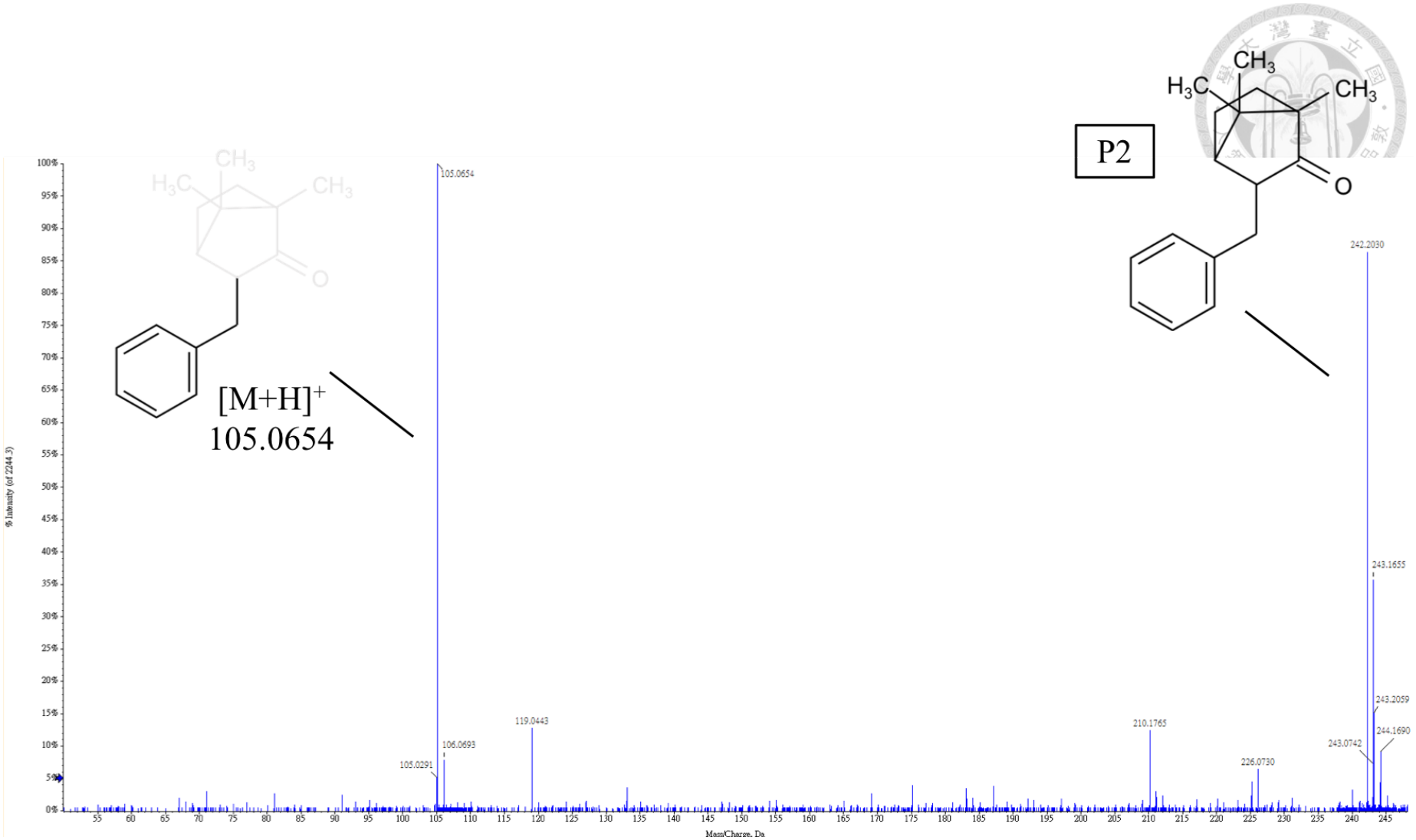

Figure S4. Mass spectrum of P2

doi:10.6342/NTU201901036

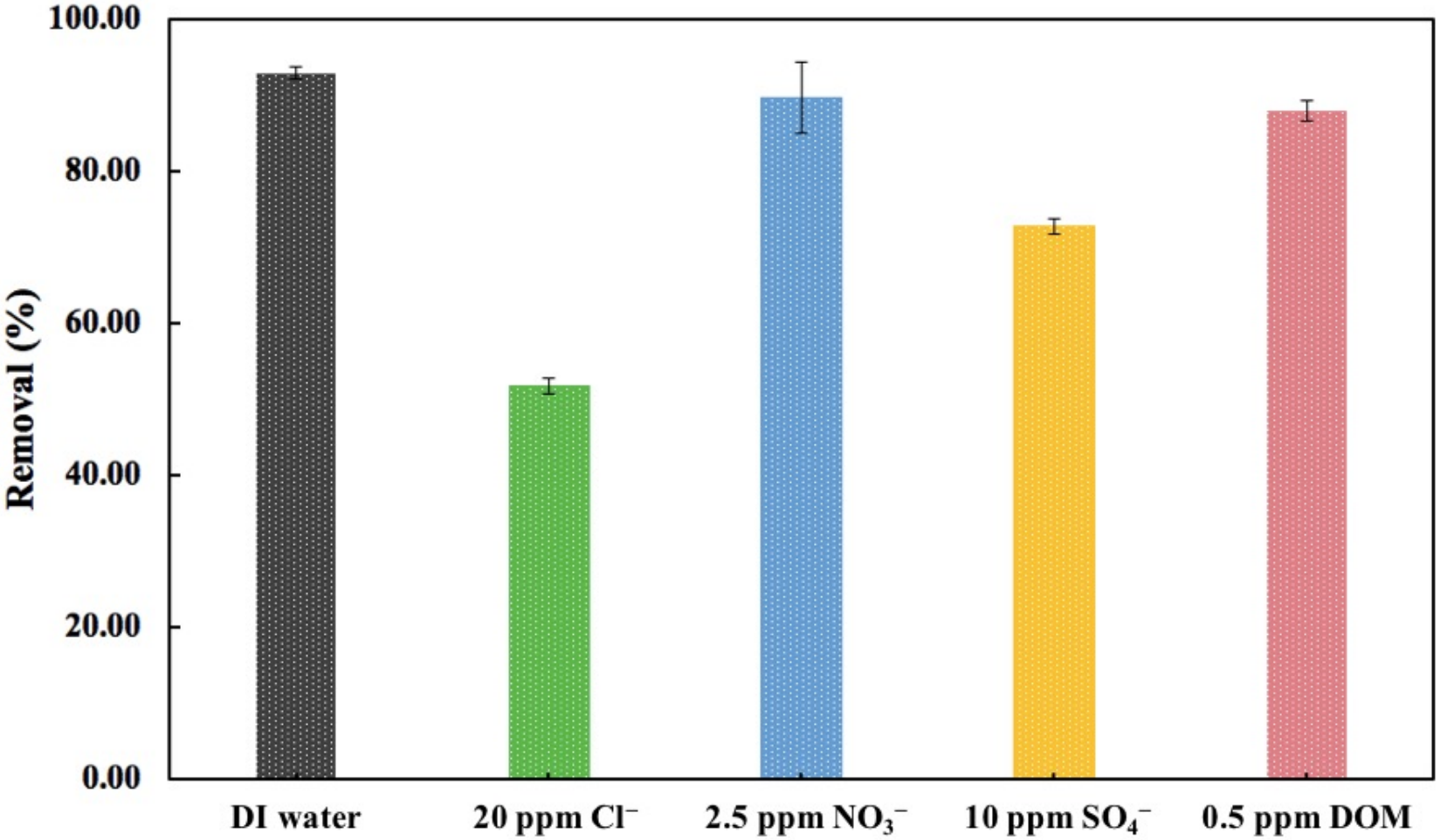

Figure S5. Removal of 4-MBC in DI water in the presence of different inorganic anions.

doi:10.6342/NTU201901036